Available online at www.sciencedirect.com

ScienceDirect

Solid Earth Sciences 1 (2016) 28–47

www.elsevier.com/locate/SESCI

Anhydrous ringwoodites in the mantle transition zone: Their bulk modulus, solid solution behavior, compositional variation, and sound velocity feature

Xi Liu [a,b,*], Zhihua Xiong [a,b], Linlin Chang [c], Qiang He [a,b], Fei Wang [a,b], Sean R. Shieh [d], Chunming Wu [c], Baosheng Li [e], Lifei Zhang [a,b]

[a] Key Laboratory of Orogenic Belts and Crustal Evolution, MOE, Peking University, Beijing 100871, China
[b] School of Earth and Space Sciences, Peking University, Beijing 100871, China
[c] College of Earth Science, University of Chinese Academy of Sciences, Beijing 100049, China
[d] Department of Earth Sciences, University of Western Ontario, London, Ontario, N6A 5B7, Canada
[e] Mineral Physics Institute, State University of New York, Stony Brook, NY 11794, USA

Available online 19 October 2015

Abstract

The isothermal bulk moduli of anhydrous Mg_2SiO_4-ringwoodite (Rw) and Fe_2SiO_4-Rw, and other 4−2 oxide spinels at ambient *P-T* condition have been evaluated, and empirically fitted to a model as $K_{T0} = 270.8(300) + 0.343(59)*V_0 + 23.04(269)*EN_{\text{-total}}$, where K_{T0} is the isothermal bulk modulus in GPa, V_0 the unit-cell volume in Å^3 and $EN_{\text{-total}}$ the electronegativity total of all cations in the chemical formula. This model well reproduces all data used in its calibration, and may be used to predict the K_{T0} of other 4−2 oxide spinels. Combined with the generally linear volume−composition relationship of the Rw solid solutions along the join Mg_2SiO_4−Fe_2SiO_4, this model leads to a much smaller composition effect on the K_{T0}: $K_{T0} = 185.0(1) + 7.0(1)*X_{Fe}$, where X_{Fe} is the atomic ratio Fe/(Fe + Mg). Furthermore, a bulk composition-independent compositional variation with *P* has been disclosed for the Rw at the *P-T* conditions of the lower part of the mantle transition zone (MTZ): $X_{Fe} = 0.222(41) - 0.0053(19)*P$, with *P* in GPa. The nearly ideal mixing behavior, much smaller composition effect on the bulk modulus, and significant compositional variation of the Rw in the lower part of the MTZ substantially increase the gradients of the V_s-*P* and V_p-*P* profiles to generally match those constrained by the seismic reference models PREM and AK135. If there is any global low-*T* anomaly at the depth of 660 km, its required magnitude is most likely not larger than 200 K.

Keywords: 4-2 spinel; Bulk modulus; Compositional variation; Mantle transition zone; Ringwoodite; Solid solution behavior; Sound velocity

1. Introduction

Due to the extremely limited availability of pristine rock samples from the deep interior of the Earth, the mineralogical model for the upper mantle is usually built by comparing the elastic data of geochemically plausible minerals to the observed seismic velocity data (Weidner and Ito, 1987; Li and Liebermann, 2007; Irifune et al., 2008). Ringwoodite (Rw), with a conventionally-accepted composition of approximately $(Mg_{0.89}Fe_{0.11})_2SiO_4$, is commonly regarded as the most abundant mineral in the lower part of the mantle transition zone (MTZ) by the geological scientific community (Irifune and Ringwood, 1987; Ita and Stixrude, 1992). Since a complete series of Rw solid solutions exists between Mg_2SiO_4 and Fe_2SiO_4, compositionally characterized by the parameter $X_{Fe} = Fe/(Fe + Mg)$ (in molar units), the correlation between the elastic properties, used in the sound velocity calculation, and composition of the Rw might be important indicator to the compositional and mineralogical model of the MTZ. Many

* Corresponding author. School of Earth and Space Sciences, Peking University, Beijing 100871, China. Tel.: +86 10 62753585; fax: +86 10 62762996.
E-mail address: xi.liu@pku.edu.cn (X. Liu).
Peer review under responsibility of Guangzhou Institute of Geochemistry.

http://dx.doi.org/10.1016/j.sesci.2015.09.001

efforts, both experimental and theoretical, have thus been made to constrain the elastic features of the ringwoodites with different compositions, and significant advances have been achieved in the last half century or so (e.g., Mao et al., 1969; Sato, 1977; Weidner et al., 1984; Zerr et al., 1993; Kiefer et al., 1997; Sinogeikin et al., 1998; Nishihara et al., 2004; Higo et al., 2006; Li et al., 2006; Matsui et al., 2006; Liu et al., 2008a; Nunez Valdez et al., 2012).

Isothermal bulk modulus at ambient *P-T* condition (K_{T0}; GPa) is one of the most important elastic properties for understanding the density and sound velocity features of Earth materials at the *P-T* conditions of the Earth's interior. Although the K_{T0} value of the Mg_2SiO_4-Rw has been reasonably well determined (e.g., Weidner et al., 1984; Hazen, 1993; Li, 2003), that of the Fe_2SiO_4-Rw is still in discrepancy, ranging from 187.3(17) to 212(10) GPa (Mao et al., 1969; Nestola et al., 2010). As a result, the dependence of the K_{T0} on the X_{Fe} of the Rw, varying from ~15 to 36 GPa/X_{Fe} (Weidner et al., 1984; Sinogeikin et al., 1998), is currently still a topic to debate. Another potential compositional factor which may strongly affect the bulk modulus of the Rw is its water content (e.g., Inoue et al., 1998; Ye et al., 2012). Although Rw can host up to ~2.7 wt% water (Kohlstedt et al., 1996; Bolfan-Casanova et al., 2000), it may be nearly anhydrous in the MTZ since recent studies using seismicity (Green et al., 2010), electromagnetic induction (Kelbert et al., 2009), electronic conductivity measurement (Yoshino et al., 2008), and sound velocity analysis (Mao et al., 2012) suggested that the water content in the MTZ probably does not exceed 0.1 wt%. On the other hand, the only terrestrial occurrence of Rw observed as inclusion in a diamond from Brazil indicates ~1 wt% water in the MTZ (Pearson et al., 2014), although it remains unclear whether this phenomenon has global implication or not.

Many advanced experimental methods such as direct high-*P* compression, ultrasonic measurement and Brillouin spectroscopy have been used to determine the isothermal bulk modulus of the Rw, and extensive and invaluable knowledge has been obtained. Direct high-*P* compression is commonly carried out by using a diamond-anvil cell (DAC) with a hydrostatic (usually $P < 10$ GPa) or quasihydrostatic ($P > 10$ GPa) pressure state since most liquid pressure media solidify at pressures lower than ~10 GPa (Klotz et al., 2009; Liu et al., 2011a). Due to the large isothermal bulk modulus of the Rw (~200 GPa), a hydrostatic pressure of about 10 GPa can press the Rw to about 95% of its ambient volume only, leading to relatively low accuracy in the determined isothermal bulk modulus. Ultrasonic measurement is intrinsically precise when single crystal or polycrystalline sample with homogeneous grain size, random grain orientation and full density (or zero porosity) is used (Sato, 1977; Liu et al., 2011b). Further, ultrasonic measurements can now be conducted at pressures higher than 3 GPa (Li et al., 1996, 1998; Li, 2003), at which a full elimination of any residual micropores and microcracks in the studied samples has been demonstrated (Liebermann, 1975; Liebermann et al., 1977; Rigden and Jackson, 1991). Ideally, Brillouin spectroscopy measurements can fully constrain the elastic tensors of a phase (Weidner et al., 1984; Wang et al., 2003a). Other experimental methods have been used as well; for a recent review, see Li and Liebermann (2014). On the other hand, it is well known that there are some specific difficulties with the synthetic Rw samples. Ringwoodites synthesized at different *P-T* conditions with different experimental durations might contain different amounts and types of defects (Smyth et al., 2003), and attain different magnitudes of order-disorder phenomenon (Hazen et al., 1993; Kudoh et al., 2000; O'Neill et al., 2003). They might have different quantities of contaminant water in their structures (Higo et al., 2006), since hydrogen can easily penetrate through most experimental capsule materials (Liu et al., 2006) and subsequently enter the Rw structure. If the dependence of the isothermal bulk modulus of the Rw on the X_{Fe} variable is relatively small, which is probably the case (Mao et al., 1969; Finger et al., 1986), all these experimental complexities then would add together to prevent a very accurate determination of this dependence and lead to controversial results (Sinogeikin et al., 1998; Higo et al., 2006).

One way around this problem is to build an empirical model which relates the bulk moduli to some other physical properties of some materials with the same crystal structure but different compositions (Anderson and Anderson, 1970; Duffy and Anderson, 1989). By extending the ranges of all the relevant properties, those uncertainties in the employed experimental techniques and variations of the physical and chemical states of the investigated samples become unimportant, and the correlation of the physical properties can be accurately established. Rw is crystallographically a cubic 4–2 oxide spinel ($Fd\bar{3}m$ with $Z = 8$) (Yagi et al., 1974; Sasaki et al., 1982), and shares the same crystal structure with a large number of phases such as Ni_2SiO_4-Sp (spinel), Co_2SiO_4-Sp, Mg_2GeO_4-Sp, Fe_2GeO_4-Sp, Co_2GeO_4-Sp, Mg_2TiO_4-Sp, Fe_2TiO_4-Sp, Co_2TiO_4-Sp and Zn_2TiO_4-Sp. Because of the similarity in the crystal structures, these spinels have been widely used as analogues to explore the high-*P* physical properties of Mg_2SiO_4-Rw (Mao et al., 1970; Liu et al., 1974; Liebermann, 1975; Liebermann et al., 1977; Sato, 1977; Finger et al., 1979; Weidner and Hamaya, 1983; Bass et al., 1984; Rigden et al., 1988; Rigden and Jackson, 1991).

This study aims at evaluating the isothermal bulk moduli of the Mg_2SiO_4-Rw and Fe_2SiO_4-Rw, and those cubic 4–2 oxide spinels obtained by different experimental techniques in recent years, and building an empirical model to describe the relationship between the isothermal bulk moduli and other physical properties such as the unit-cell volume and the electronegativity of the cations. It has been demonstrated that such an empirical model can reproduce well all the data used in its calibration. In addition, this model has been examined with some extra experimental data which have not been used in its construction, and satisfactory agreement has been achieved as well. To apply this model to the Rw solid solutions in the system Mg_2SiO_4–Fe_2SiO_4, a well-established volume–composition relationship is a prerequisite. We have summarized all the Rw volume-composition data reported so far, and found a nearly linear solid solution behavior for the Rw solid solutions. Eventually a much smaller composition effect on the bulk modulus of the Rw has been revealed.

Furthermore, the compositional data of the Rw reported in some high-*P* experimental studies with peridotitic mantle compositions have been carefully scrutinized. Contrary to the prevalent assumption of a constant composition, we have found that the X_{Fe} of the Rw at the *P-T* conditions of the lower part of the MTZ decreases significantly with *P* increase. Taking all these observations into account, finally, the sound velocity features of the Rw at the *P-T* conditions of the lower part of the MTZ have been explored, and their geophysical implications have been discussed in this paper.

2. A model for the bulk modulus: building techniques

The general chemical formula for the Rw and other 4–2 oxide spinels is AB_2O_4, with A being a 4+ and B a 2+ cation. The first-order crystal structural feature of these compounds is a cubic close packing array made of the oxygens, which is slightly modified by the A and B cations occupying one eighth of the tetrahedral (8a) and half of the octahedral (16d) sites, respectively. The A and B cations might partially switch their positions due to changes of temperature, pressure and composition (e.g., Wechsler et al., 1984; Liu and Prewitt, 1990; Wittlinger et al., 1998; O'Neill et al., 2003; Antao et al., 2005; Rozenberg et al., 2007; Gatta et al., 2014), and these materials become crystallographically disordered, so that a more general chemical formula can be written as $[A_{(1-i)}B_i]^{tet}[A_iB_{(2-i)}]^{oct}O_4$. If $i = 0$, the spinel has an ordered normal cation distribution ($[A]^{tet}[B_2]^{oct}O_4$, normal spinel); if $i = 1$, the spinel has an ordered inverse cation distribution ($[B]^{tet}[AB]^{oct}O_4$, inverse spinel); if $i = 2/3$, the spinel has a completely random cation distribution between the tetrahedral and octahedral sites.

The isothermal bulk moduli of the oxide spinels have been demonstrated to be primarily controlled by their volumes (Anderson and Anderson, 1970), and the values of the isothermal bulk moduli can be estimated from the crystal chemical systematics which influences the volumes (Hazen and Yang, 1999). The same phenomenon was observed for apatites in some recent studies (He et al., 2012, 2013). Besides the influence of the volume, also observed by He et al. (2013), was a possible effect of some other physical features of the cation species because the $Pb_{10}(PO_4)_6F_2$-apatite and $Sr_{10}(PO_4)_6F_2$-apatite have similar volumes but rather different bulk moduli. Following Li et al. (2011), we assume that this additional effect can be globally approximated by the electronegativity total of the cations in the crystals. Electronegativity is traditionally defined as the ability of an atom to attract or hold its valence electrons, and thus symbolic of its chemical bond. It is well known that the nature of the chemical bonds in a crystal strongly influences the crystal's ability to resist compression (Liu and Cohen, 1989), i.e., the bulk modulus within the elastic regime. Eventually we have chosen to build our empirical model with the following equation:

$$K_{T0} = a + b*V_0 + c*EN_{-total} \quad (1)$$

where K_{T0} is the isothermal bulk modulus at 1 atm and 298 K, V_0 the unit-cell volume at 1 atm and 298 K, EN_{-total} the electronegativity total of all cations, and a, b and c the fitting constants. The variable EN_{-total} is defined as:

$$EN_{-total} = \sum (C_j*EN_j) \quad (2)$$

where C_j is the number of cation j in the Sp chemical formula and EN_j the electronegativity of cation j, which is adopted from Holtzclaw and Robinson (1988). V_0 is simply an averaged value calculated from existing volume measurements for each single Sp composition.

A critical reviewing over the isothermal bulk moduli of the 4–2 oxide spinels is a prerequisite to the success of our empirical model. When an isothermal bulk modulus has been determined by multiple experimental methods, priority is given to the results constrained by the direct compression data and ultrasonic measurements, simply because the authors have more experience in them (e.g., Shieh et al., 2006; Li and Liebermann, 2007, 2014; Liu et al., 2008b, 2009, 2011a, 2011b; He et al., 2012, 2013; Chang et al., 2013; Xiong et al., 2015). If a bulk modulus has been measured by the same experimental technique for several times, the most recent values are adopted to derive an averaged value. For some spinels, only ultrasonic measurement is available, and has to be used (Liebermann, 1975; Rigden and Jackson, 1991). In these cases, the measurements with larger *P* range supersede the measurements with smaller *P* range, since higher *P* provides more chance to eliminate the residual porosity in the sample.

Certain rules apply to the volume data as well. Factors such as the order-disorder magnitude of the cations, possible water contamination absorbed from the experimental assembly, and oxidation state of the cations such as Fe, Ge and many others can affect the volume of the oxide spinels (Bartram and Slepetys, 1961; Hazen and Yang, 1999; Smyth et al., 2003; O'Neill et al., 2003; Higo et al., 2006). To minimize the effects of these factors, we only consider the volume data directly measured from the materials which were used to experimentally constrain their bulk moduli.

When examining the experimental data, we ignore the following several factors which slightly influence the value of the isothermal bulk modulus. The relative difference between the isothermal bulk modulus obtained by direct compression experiments and adiabatic bulk modulus (K_{S0}) determined by either ultrasonic measurements or Brillouin spectroscopic data, $(K_{S0} - K_{T0})/K_{T0} = \alpha\gamma T$ where α is the volumetric thermal expansion coefficient (averagely 3.5×10^{-5} K^{-1}; see Table 4 in Wang et al. (2012)) and γ the Grüneisen parameter (commonly less than 2; e.g., Chopelas and Hofmeister (1991), Hofmeister and Mao (2001), Wang et al. (2002a, 2003b) and Yong et al. (2012)), is usually in the range of 2% at ambient *P-T* condition, leading to an absolute difference of ~4 GPa only (K_{T0} approximating ~200 GPa; Finger et al. (1986)). The correlation between the isothermal bulk modulus and its first *P* derivative (K_{T0}'), although greater than 95%, is not considered as well, simply because K_{T0}' was either not constrained in most cases (K_{T0}' fixed as 4 then) or usually showed to have a small deviation from 4 in the cases with full experimental determination (Rigden et al., 1988; Li, 2003; Nishihara et al.,

Table 1
Volume and bulk modulus of Rw and some 4–2 oxide spinels at 1 atm and 300 K.

Formula	V_0 (Å^3)	K_{T0} (GPa)	K_{T0}'	Sample[a]	Technique[b]	Experimental note[c]	Reference
Mg_2SiO_4	526.5(2)	213(10)	4(fixed)	25[d]/1273/G	XRD; ~9	Single-stage MA	Mizukami et al. (1975)
	527.1(1)	184(6)	4.8(fixed)	20/1673/S	XRD; ~5	DAC; PM (4:1 ME)	Hazen (1993)
	526.7(3)	182(3)	4.2(3)	19.5/1173/G	XRD; ~30	DAC; PM (Ne)	Meng et al. (1994)
	–	185(2)	4.5(2)	20/1473/G	US; ~12	Two-stage MA	Li (2003)
	–	185(3)	4.4(2)	19/1473/G	US; ~14	Two-stage MA	Higo et al. (2006)
	525.3	184(3)	–	22/2473/S	BS; 1 atm		Weidner et al. (1984)
	525.2	185(3)	–	–/–/S	BS; 1 atm		Jackson et al. (2000)
	–	190	4.19	–	Theory		Kiefer et al. (1997)
	–	181.0(3)	4.10(2)	–	Theory		Matsui (1999)
	–	173	–	–	Theory		Piekarz et al. (2002)
	–	173	–	–	Theory		Li et al. (2006)
	–	184.4	–	–	Theory		Nunez Valdez et al. (2012)
Fe_2SiO_4	558.3(17)	212(10)	4(fixed)	~6/~1100/G	XRD; ~25	DAC; PM (NaCl)	Mao et al. (1969)
	558.7(20)	189(12)	4(fixed)	~/~1100/G	XRD; ~7	DAC; PM (4:1 ME)	Wilburn and Bassett (1976)
	–	197(2)	4(fixed)	–/–/G	XRD; ~8	CP; PM (4:1 ME)	Sato (1977)
	558.7(2)	196(6)	4(fixed)	7.5/1773/S	XRD; ~4	DAC; PM (WG)	Finger et al. (1979)
	558.8(1)	207(3)	4.8(fixed)	5.5/1673/S	XRD; ~5	DAC; PM (4:1 ME)	Hazen (1993)
	559.38(7)	187.3(17)	5.5(4)	7/1373/S	XRD; ~10	DAC; PM (4:1 ME)	Nestola et al. (2010)
	–	202(4)	4(fixed)	–/–/G	XRD; ~25	DAC; PM (NaCl)	Armentrout and Kavner (2011)
	–	212	–	7.5/1173/G	US; 0.6	Porosity: 2.0%	Mizutani et al. (1970)
	558.30	193	–	5.8/1273/G	US; 0.75	Porosity: 3.5%	Liebermann (1975)
	–	201	5.59	5.8/1273/G	US; 3	Porosity: 3.5%	Rigden and Jackson (1991)
	–	204.5(7)	4.3(3)	7.4/1173/G	US; ~6.5	CP	Liu et al. (2008a)
Ni_2SiO_4	520.4(16)	214(7)	4(fixed)	3.2/1173/G	XRD; ~30	DAC; PM (NaCl)	Mao et al. (1970)
	–	223(2)	4(fixed)	–/–/G	XRD; ~8	CP; PM (4:1 ME)	Sato (1977)
	520.5(1)	227(4)	4(fixed)	5.5/1673/S	XRD; ~4	DAC; PM (ME[e])	Finger et al. (1979)
	521.13(8)	233(2)	4.8(fixed)	7.5/1773/S	XRD; ~5	DAC; PM (ME)	Hazen (1993)
	520.2(2)	226(2)	–	~4/~1423/S	BS; 1 atm		Bass et al. (1984)
	520.57	216	–	5.6/1373/G	US; ~0.75	Porosity: 4.3%	Liebermann (1975)
Co_2SiO_4	539.2(3)	210(6)	4.0(6)	–/–/G	XRD; ~28	DAC; PM (NaCl)	Liu et al. (1974)
	–	206(2)	4(fixed)	–/–/G	XRD; ~8	CP; PM (4:1 ME)	Sato (1977)
Mg_2GeO_4	560.5	179	–	0.2/~1023/S	BS; 1 atm	Inclusions/defects	Weidner and Hamaya (1983)
	562.55	179	4.22[f]	3.5/1473/G	US; ~0.75	Porosity: 1.4%	Liebermann (1975)
Fe_2GeO_4	595.09	196	4.86	3.0/1113/G	US; ~3	Porosity: 1.4%	Rigden and Jackson (1991)
	595.09	185	–	3.0/1113/G	US; ~0.75	Porosity: 1.4%	Liebermann (1975)
Co_2GeO_4	576.37	192	5.59	3.0/1273/G	US; ~3	Porosity: 1.1%	Rigden and Jackson (1991)
	576.37	196	–	3.0/1273/G	US; ~0.75	Porosity: 1.1%	Liebermann (1975)
Ni_2GeO_4	555.64	203	4.78	3.0/1273/G	US; ~3	Porosity: 0.9%	Rigden and Jackson (1991)
	555.64	184	–	3.0/1273/G	US; ~0.75	Porosity: 0.9%	Liebermann (1975)
Mg_2TiO_4	601.21	152 (7)	–	0.5/1773/G	US; ~0.75	Porosity: 1.4%	Liebermann et al. (1977)
Fe_2TiO_4	624.35(4)	250.8(25)	4(fixed)	–/–/S	XRD; ~8.8	DAC; PM (MEW)	Yamanaka et al. (2009)
	620.59(5)	250.8(25)	4(fixed)	–/–/G	XRD; ~7.1	DAC; PM (Ne)	Yamanaka et al. (2013)
	–	121(2)	–	–/–/S	US; 1 atm		Syono et al. (1971)
Co_2TiO_4	601.07	162(9)	–	2.0/1273/G	US; ~0.75	Porosity: 3.5%	Liebermann et al. (1977)
Zn_2TiO_4	604.7(2)	162(11)	4(fixed)	1/1473/G	XRD; ~28	DAC; NPM	Wang et al. (2002b)

[a] Sample synthesized at certain P (GPa) and T (K), and then used as starting material in later measurement in the form of finely Ground powder (G) or Single crystal (S).
[b] XRD, X-ray diffraction; US, Ultrasonic measurement; BS, Brillouin spectroscopy; number indicating the maximum P (GPa) in the measurements.
[c] MA, multi-anvil press; DAC, diamond-anvil cell; CP, cubic press; PM, pressure medium; NPM, no pressure medium; 4:1 ME, 4:1 methanol–ethanol mixture; Ne, neon; WG, water–glycerin mixture; MEW, methanol–ethanol–water mixture; Porosity, porosity at 1 atm.
[d] Pressure slightly overestimated.
[e] Water + glycerin (WG) also used.
[f] Value from Rigden and Jackson (1991).

2004; Higo et al., 2006; Matsui et al., 2006; Higo et al., 2008); in the latter cases, the deviation is commonly less than 0.5, which leads to an uncertainty of <5 GPa in the bulk modulus of the 4–2 oxide spinels (Liu et al., 1974). The effect of cation disorder on the bulk modulus is negligible (less than 3 GPa), taking into account the facts that the degree of cation disorder of the 4–2 oxide spinels is usually less than 10% (e.g., Yagi et al., 1974; O'Neill and Navrotsky, 1983; Yamanaka, 1986; Hazen et al., 1993; Panero, 2008) and that the difference of the bulk moduli between the normal and inverse 4–2 oxide spinels with the same composition is expected to be ~17% (Hazen and Yang, 1999) or even less (Kiefer et al., 1999; Panero, 2008). Direct high-P compression experiments on two 2–3 $[Mg_{(1-i)}Al_i][Mg_iAl_{(2-i)}]O_4$ spinels (i = 0.15 and 0.27, respectively) demonstrated essentially identical bulk moduli [193(1) versus 192(1) GPa], and thus fully supported this

Table 2
K_{T0} of Rw and other 4–2 spinels at ambient *P-T* condition.[a]

Composition	V_0 (Å^3)	$EN_{\text{-total}}$[b]	$K_{T0\text{-exp}}$ (GPa)	$K_{T0\text{-cal}}$ (GPa)	Difference (GPa)
Data for model-building					
Mg_2SiO_4	526.3(7)	4.1(1)	184(1)	185	1
Fe_2SiO_4	558.6(4)	4.9(1)	200(8)	192	−8
Ni_2SiO_4	520.6(4)	5.3(1)	223(7)	214	−9
Co_2SiO_4	539.2(3)	5.1(1)	210(6)	203	7
Mg_2GeO_4	561.5(14)	4.4(1)	179(6)[c]	180	1
Fe_2GeO_4	595.1(30)[d]	5.2(1)	196(6)[c]	186	−10
Co_2GeO_4	576.37(29)[d]	5.4(1)	192(6)[c]	198	6
Ni_2GeO_4	555.64(28)[d]	5.6(1)	203(6)[c]	209	6
Mg_2TiO_4	601.21(30)[d]	3.7(1)	152(7)	150	−2
Co_2TiO_4	601.07(30)[d]	4.7(1)	162(9)	173	11
Zn_2TiO_4	604.68(24)	4.7(1)	162(11)	172	10
Data for model-checking; Rw along the Mg_2SiO_4–Fe_2SiO_4 join					
X_{Fe} = 0.9	556(17)	4.8(1)	196(10)[c]	191	−5
X_{Fe} = 0.8	552.2(17)	4.7(1)	208(10)[c]	191	−17
X_{Fe} = 0.8	552.89(19)	4.7(1)	205(2)[f]	190	−15
X_{Fe} = 0.78	552.45(9)	4.7(1)	205(2)[f]	190	−15
X_{Fe} = 0.6	546.61(14)	4.6(1)	203(2)[f]	189	−14
X_{Fe} = 0.5	545.3(3)	4.5(1)	191(2)[g]	187	−4
X_{Fe} = 0.4	535.59(40)	4.4(1)	183(5)[h]	189	6
X_{Fe} = 0.25	535.0(2)	4.3(1)	193(3)[i]	186	−7
X_{Fe} = 0.2	531.44(15)	4.3(1)	189.7[j]	187	−3
X_{Fe} = 0.2	536.3(3)	4.3(1)	187(2)[g]	185	−2
X_{Fe} = 0.09	526.2(4)	4.2(1)	188(3)[k]	186	−2
X_{Fe} = 0.09	527.83(7)	4.2(1)	187[l]	186	−1
X_{Fe} = 0.09	528.43(18)	4.2(1)	184.1(6)[m]	186	2
X_{Fe} = 0	526.7(3)	4.1(1)	185(2)[g]	185	0

[a] K_{T0}' is not considered; see text for the relevant discussion.
[b] Error assumed to be 0.1.
[c] Error assumed to be 6 GPa.
[d] Error assumed to be 0.05%.
[e] Mao et al. (1969).
[f] Hazen (1993).
[g] Higo et al. (2006); small amounts of H_2O (~550 ppm) were detected in the samples.
[h] Zerr et al. (1993).
[i] Sinogeikin et al. (1997).
[j] Matsui (1999).
[k] Sinogeikin et al. (1998).
[l] Nishihara et al. (2004).
[m] Higo et al. (2008).

argument (Nestola et al., 2007). Since significant non-stoichiometry has not been experimentally observed for the anhydrous ringwoodites (Irifune and Ringwood, 1987; Irifune, 1994; Wood, 2000; Hirose, 2002), furthermore, we focus on the experimental data collected from the stoichiometric 4–2 oxide spinels and ignore the effect of non-stoichiometry on the bulk moduli. Bear in mind though that the experimental studies on a 2–3 spinel ($Mg_{0.4}Al_{2.4-0.2}O_4$; Nestola et al., 2009a, 2009b) indicated a relatively strong effect of the non-stoichiometry (an ~11.5% reduction of the bulk modulus in this case).

3. A model for the bulk modulus: evaluating input data

The isothermal bulk moduli of 12 4–2 oxide spinels at ambient *P-T* condition have been experimentally measured, and the corresponding experimental details are summarized in

Table 3
V_0-X_{Fe} data for the anhydrous Rw at ambient *P-T* condition.

X_{Fe}	V_0 (Å^3)	$EN_{\text{-Total}}$[a]	Ref.
1	558.3(17)	4.9(1)	Mao et al. (1969)
1	558.7(20)	4.9(1)	Wilburn and Bassett (1976)
1	558.7(2)	4.9(1)	Finger et al. (1979)
1	558.8(1)	4.9(1)	Hazen (1993)
1	559.38(7)	4.9(1)	Nestola et al. (2010)
1	557.69(2)	4.9(1)	Nestola et al. (2011a)
1	558.3(3)[b]	4.9(1)	Liebermann (1975)
1	559.8(1)	4.9(1)	Ding et al. (1990)
0.9	554.8(1)	4.8(1)	Akimoto and Fujisawa (1968)
0.9	556.0(2)	4.8(1)	Mao et al. (1969)
0.8	551.8(2)	4.7(1)	Akimoto and Fujisawa (1968)
0.8	552.2(2)	4.7(1)	Mao et al. (1969)
0.8	551.66(30)	4.7(1)	Akaogi et al. (1989)
0.8	552.89(19)	4.7(1)	Hazen (1993)
0.78	552.45(9)	4.7(1)	Hazen (1993)
0.78	552.45(9)	4.7(1)	Hazen (1993)
0.7	549.2(1)	4.7(1)	Akimoto and Fujisawa (1968)
0.6	546.3(1)	4.6(1)	Akimoto and Fujisawa (1968)
0.6	545.28(30)	4.6(1)	Akaogi et al. (1989)
0.6	546.61(14)	4.6(1)	Hazen (1993)
0.6	546.42(12)	4.6(1)	Hazen (1993)
0.4	538.51(30)	4.4(1)	Akaogi et al. (1989)
0.4	535.59(40)	4.4(1)	Zerr et al. (1993)
0.25	535.0(2)	4.3(1)	Sinogeikin et al. (1997)
0.2	531.07(30)	4.3(1)	Akaogi et al. (1989)
0.2	531.44(15)	4.3(1)	Matsui et al. (2006)
0.09	526.2(4)	4.2(1)	Sinogeikin et al. (1998)
0.09	529.00(11)	4.2(1)	Nishihara et al. (2004)
0.09	528.32(12)	4.2(1)	Nishihara et al. (2004)
0.09	528.43(18)	4.2(1)	Nishihara et al. (2004)
0.09	529.7(26)[c]	4.2(10)	Higo et al. (2008)
0	526.5(2)	4.1(1)	Mizukami et al. (1975)
0	525.3(3)[b]	4.1(1)	Weidner et al. (1984)
0	525.09(30)	4.1(1)	Akaogi et al. (1989)
0	527.10(8)	4.1(1)	Hazen (1993)
0	526.6(2)	4.1(1)	Hazen (1993)
0	526.54(13)	4.1(1)	Hazen (1993)
0	526.7(3)	4.1(1)	Meng et al. (1994)
0	525.2(3)[b]	4.1(1)	Jackson et al. (2000)
0	524.8(1)	4.1(1)	Katsura et al. (2004)

[a] Error assumed to be 0.1.
[b] Error assumed to be 0.05%.
[c] Error calculated according to the 0.5% porosity in the sample.

Table 4
Effect of X_{Fe} on some elastic moduli of Rw along the join Mg_2SiO_4–Fe_2SiO_4 based on a linear fit.[a]

	a	b	Source of data
K_{S0}[b]	184	15	Weidner et al. (1984)
	184	36	Sinogeikin et al. (1998)
	184	16	Higo et al. (2006)
	184.7	18.1	Liu et al. (2008a)
	185.0(1)	7.0(1)	This study
G_0	119	−41	Weidner et al. (1984)
	120	−25	Sinogeikin et al. (1998)
	124	−45	Higo et al. (2006)
	118.7	−41.4	Liu et al. (2008a)

[a] K_{S0} (G_0) = a + b × X_{Fe}; K_{S0}, G_0, a and b are in GPa.
[b] Difference between K_{S0} and K_{T0} is ignored; see text for the relevant discussion.

Table 1. Since our major interest here is to probe the composition dependence of the bulk modulus of the ringwoodites by extending the variation ranges of the bulk modulus and other physical properties, any data about the Rw solid solutions along the Mg_2SiO_4–Fe_2SiO_4 join would not help and are not used in the model-building process.

3.1. Mg_2SiO_4-Sp (or Mg_2SiO_4-Rw)

Mg_2SiO_4-Sp was firstly synthesized by Suito (1972), with its crystallographic details later investigated by Sasaki et al. (1982). Although the difference in the scattering factors of Mg and Si was small and a precise estimate of their site occupancies was difficult, Hazen et al. (1993) successfully demonstrated that Mg_2SiO_4-Sp was generally a normal spinel with a limited amount of Si (~4%) entering the octahedral sites.

The bulk modulus of Mg_2SiO_4-Sp has been determined in many studies with different techniques (Table 1). Mizukami et al. (1975) pioneered in this research field, but their result was ~15% larger than all other experimental estimates, presumably due to some special technique difficulties such as the prolonged X-ray diffraction data-collecting time and complicated mechanic behavior of the experimental assemblage used on the single-stage multi-anvil (MA) press. Later compression studies suggested that the bulk modulus of Mg_2SiO_4-Sp was averagely 183(1) GPa at ambient *P-T* condition (Hazen, 1993; Meng et al., 1994). Experimental studies using other techniques such as Brillouin spectroscopy and ultrasonic measurement generated a bulk modulus of 185(1) GPa for Mg_2SiO_4-Sp (300 K; Weidner et al. (1984), Jackson et al. (2000), Li (2003) and Higo et al. (2006)), in excellent agreement with the compression result. In comparison, recent theoretical investigations produced more scattering results, with some suggesting a value of 185 (5) GPa (Kiefer et al., 1997; Matsui, 1999; Nunez Valdez et al., 2012) and some suggesting a much lower value of 173 GPa (Piekarz et al., 2002; Li et al., 2006). It follows that the averaged result from those experimental studies (excluding Mizukami et al. (1975)), 184(1) GPa, should be a good estimate of the bulk modulus of Mg_2SiO_4-Sp at ambient *P-T* condition.

The unit-cell volume of Mg_2SiO_4-Sp at 1 atm and 300 K has been calculated as 526.3(7) $Å^3$ from the data listed in Table 1.

3.2. Fe_2SiO_4-Sp (or Fe_2SiO_4-Rw)

Fe_2SiO_4-Sp was firstly synthesized by Ringwood (1958). It is stable from ~7 to 18 GPa and breaks down to wüstite and stishovite at higher pressure (Ohtani, 1979). Detailed crystal structure studies by Yagi et al. (1974) and Yamanaka (1986) suggested that Fe_2SiO_4-Sp was essentially a normal spinel (up to 2% Si occurring on the octahedral sites). On the other hand, a powder X-ray diffraction study by Ding et al. (1990) suggested that up to ~38% Si atoms were octahedrally coordinated. No much information about the charge state of iron in the investigated samples was available.

The bulk modulus of Fe_2SiO_4-Sp has been determined by many research groups. Its values obtained by several direct compression experiments varied from 187(2) to 212(10) GPa, with an average of 199(9) GPa (Mao et al., 1969; Wilburn and Bassett, 1976; Sato, 1977; Finger et al., 1979; Hazen, 1993; Nestola et al., 2010; Armentrout and Kavner, 2011). On the other hand, the bulk modulus of Fe_2SiO_4-Sp determined by ultrasonic measurements (Mizutani et al., 1970; Liebermann, 1975; Ridge and Jackson, 1991; Liu et al., 2008a) was averagely 203(8), which was generally in agreement with the result from the compression experiments. Considering the experimental uncertainties, we assume that the averaged result from all these experimental studies, 200(8) GPa, is a reasonably good estimate of the bulk modulus of Fe_2SiO_4-Sp.

The unit-cell volume of Fe_2SiO_4-Sp at 1 atm and 300 K has been calculated as 558.6(4) $Å^3$ from the data listed in Table 1.

3.3. Ni_2SiO_4-Sp

Ni_2SiO_4-Sp was firstly synthesized by Ringwood (1962). It is stable in the pressure interval of ~3–28 GPa and breaks down to a mixture of bunsenite (NiO) and stishovite (SiO_2) at higher pressures (e.g., Akimoto et al., 1965; Liu, 1975a; Ito, 1975). Detailed single-crystal X-ray diffraction studies by Yagi et al. (1974) and Yamanaka (1986) suggested that Ni_2SiO_4-Sp was essentially a normal spinel. In contrast, a powder X-ray diffraction study by Ma (1975) demonstrated that up to 8(6)% Si atoms were octahedrally coordinated.

The bulk modulus of Ni_2SiO_4-Sp has been determined in many experimental studies with a range of techniques such as high-*P* compression, ultrasonic velocity measurement and Brillouin spectroscopy (Mao et al., 1970; Liebermann, 1975; Sato, 1977; Finger et al., 1979; Bass et al., 1984; Hazen, 1993). The values obtained in these studies (from 216 to 233 GPa) were in good agreement, with an averaged value of 223(7) GPa.

The unit-cell volume of Ni_2SiO_4-Sp at 1 atm and 300 K has been calculated as 520.6(4) $Å^3$ from the data listed in Table 1.

3.4. Co_2SiO_4-Sp

Co_2SiO_4-Sp was firstly synthesized by Ringwood (1963). It is stable in the pressure interval of ~6–17 GPa and breaks down to a mixture of CoO (rocksalt structure) and SiO_2 (stishovite) at higher pressures (Akimoto and Sato, 1968; Liu, 1975b; Ito, 1975). Morimoto et al. (1974) investigated its crystal structure using single crystal X-ray diffraction method, and found that it was generally a normal spinel (up to ~3% Si occurring on the octahedral sites).

The bulk modulus of Co_2SiO_4-Sp has been experimentally determined as 210(6) GPa by Liu et al. (1974) and as 206(2) GPa by Sato (1977). Since the latter did not report the unit-cell volume, the K_{T0} value from the former is preferred in this study. Anyhow, the results from these two studies were in excellent agreement.

The unit-cell volume of Co_2SiO_4-Sp at 1 atm and 300 K used in our model-building is from Liu et al. (1974), as listed in Table 1.

3.5. Mg_2GeO_4-Sp

Mg_2GeO_4-Sp is stable at atmospheric pressure below 1083 K and at high pressures at least up to 7 GPa (Dachille and Roy, 1960; Miyamoto et al., 1978). According to the neutron powder diffraction study by Von Dreele et al. (1977), it is a normal spinel. In contrast, powder X-ray diffraction analysis by Liebermann et al. (1977) demonstrated up to 8(4)% octahedrally-coordinated Si atoms in the Mg_2GeO_4-Sp.

The Brillouin spectroscopy data from Weidner and Hamaya (1983) suggested that the bulk modulus of Mg_2GeO_4-Sp at ambient T was about 179 GPa.

The unit-cell volume of Mg_2GeO_4-Sp at 1 atm and 300 K has been calculated as 561.5(14) $Å^3$ from the data listed in Table 1.

3.6. Fe_2GeO_4-Sp

Under appropriate oxygen fugacity, Fe_2GeO_4-Sp is stable both at atmospheric pressure and at high pressures (Hariya and Wai, 1970). It is a fully-ordered normal spinel, as suggested by the single-crystal X-ray diffraction study of Welch et al. (2001) (natural sample).

The ultrasonic measurements up to ~3 GPa by Rigden and Jackson (1991) suggested that the bulk modulus of Fe_2GeO_4-Sp was about 196 GPa, which has been used in this study. No direct compression experiment has been performed with Fe_2GeO_4-Sp to constrain its bulk modulus.

3.7. Co_2GeO_4-Sp

Co_2GeO_4-Sp is stable at atmospheric pressure and in a wide range of P-T conditions, with its high-P stability limit undefined yet (Liu, 1976a; Inagaki et al., 1977; Ito and Matsui, 1979). At ~25 GPa and 1673–2073 K, the stable phase assemblage for the Co_2GeO_4 composition is CoO (rocksalt structure) + GeO_2 (rutile structure). Although no single-crystal X-ray data are available, existing powder X-ray diffraction data suggest that coexisting Co and Ge in the same tetrahedral sites are unfavorable (Furuhashi et al., 1973a), and Co_2GeO_4-Sp is generally a normal spinel (Furuhashi et al., 1973b).

The ultrasonic measurements up to ~3 GPa by Rigden and Jackson (1991) suggested that the bulk modulus of Co_2GeO_4-Sp was about 192 GPa, which has been adopted in this study. No direct compression experiment has been performed with Co_2GeO_4-Sp to constrain its bulk modulus.

3.8. Ni_2GeO_4-Sp

Ni_2GeO_4-Sp is stable in a wide range of P-T conditions, with its exact phase stability field undefined yet (Lin, 1976a; Ito and Matsui, 1979). At ~25 GPa and 1673–2073 K, the stable phase assemblage for the Ni_2GeO_4 composition is NiO (rocksalt structure) + GeO_2 (rutile structure). Although no detailed crystal structural data have been reported, Ni_2GeO_4-Sp is mostly likely a normal spinel, especially for temperatures below 1273 K (Datta and Roy, 1967).

The ultrasonic measurements up to ~3 GPa by Rigden and Jackson (1991) suggested that the bulk modulus of Ni_2GeO_4-Sp was about 203 GPa, which has been used in this study. No direct compression experiment has been performed with Ni_2GeO_4-Sp to constrain its bulk modulus.

3.9. Mg_2TiO_4-Sp

Mg_2TiO_4-Sp is stable from 1 atm to ~1 GPa (Akimoto and Syono, 1967), and breaks down to MgO (rocksalt structure) and $MgTiO_3$ (ilmenite structure). Its crystal structure has been studied by powder neutron diffraction, powder X-ray diffraction and single-crystal X-ray diffraction (Wechsler and Von Dreele, 1989; Millard et al., 1995; Sawada, 1996), which suggested an inverse spinel structure. O'Neill et al. (2003) investigated the dependence of its cation disordering on temperature, and found that it had a completely inverse cation distribution at temperature below ~1127 K and became slightly disordered at higher temperatures (~4% Ti entering the tetrahedral sites at 1689 K).

The bulk modulus of Mg_2TiO_4-Sp has been constrained as 152(7) GPa by ultrasonic velocity data up to 0.75 GPa only (Liebermann et al., 1977). More investigation is necessary.

3.10. Fe_2TiO_4-Sp

Fe_2TiO_4-Sp is stable from 1 atm to about 4 GPa (Akimoto and Syono, 1967). In general, it can be regarded as an inverse spinel. According to Wechsler et al. (1984) and Yamanaka et al. (2013), Ti only occurs on the octahedral sites, suggesting a completely ordered structure. In contrast, Forster and Hall (1965) and Sedler et al. (1994) demonstrated that a small amount of Ti (up to 18%) might occupy the tetrahedral sites.

Recently Yamanaka et al. (2009, 2013) carried out compression experiments up to ~9 GPa, which constrained the bulk modulus of Fe_2TiO_4-Sp as ~250.8(25) GPa. They used either ethanol-methanol-water mixture or neon as the pressure medium to secure a quasi-hydrostatic environment in their DAC experiments (Klotz et al., 2009), so that a high quality in their volume data at high pressures should have been expected. Unfortunately, their result was too different to an earlier estimate based on some ultrasonic measurements (121(2) GPa; Syono et al. (1971); Liebermann et al. (1977)). Consequently, the data for Fe_2TiO_4-Sp have been left out in building our empirical model.

3.11. Co_2TiO_4-Sp

Co_2TiO_4-Sp is stable from 1 atm to ~3 GPa (Akimoto and Syono, 1967), and breaks down to CoO (rocksalt structure) and $CoTiO_3$ (ilmenite structure). Although its detailed crystal

structure is unavailable, it is usually regarded as an inverse spinel (Sakamoto, 1962; Dube and Darshane, 1991).

The bulk modulus of Co_2TiO_4-Sp was constrained as 162(9) GPa by ultrasonic velocity data up to 0.75 GPa only (Liebermann et al., 1977). More investigation is apparently favorable.

3.12. Zn_2TiO_4-Sp

Zn_2TiO_4-Sp is usually regarded as an inverse spinel (Verwey and Heilmann, 1947). When synthesized at temperatures close to ~1473 K, it is completely inverse whereas it should become slightly disordered if the synthesizing temperature goes higher (Bartram and Slepetys, 1961; Millard et al., 1995).

Wang et al. (2002b) conducted their sintering experiment at 1473 K, so that their Zn_2TiO_4-Sp should be nearly fully inverse. Their compression experiments constrained the bulk modulus of Zn_2TiO_4-Sp as 162(11) GPa. Since no pressure medium was used in their room-T DAC experiments, this value should be viewed with reserve.

4. A model for the bulk modulus: building and examining

As revealed in the previous section, 11 sets of bulk modulus-volume data are available for the calibration of our empirical model (Table 2). The range of the K_{T0} values, from 152 to 223 GPa, is about 4.4 times that of the K_{T0} values of Mg_2SiO_4-Sp and Fe_2SiO_4-Sp whereas the range of the unit-cell volume values, from 520.6 to 604.68 Å^3, is about 2.6 times that of the volume values of Mg_2SiO_4-Sp and Fe_2SiO_4-Sp.

A weighted multiple linear least-squares fit to the data has been conducted. The data without uncertainties are weighted by assuming (1) a 0.05% uncertainty in the unit-cell volume, (2) a 0.1 uncertainty in the $EN_{\text{-total}}$, and (3) a 6 GPa uncertainty in the bulk modulus of the germanate spinels (Table 2). These germanate spinels were investigated by using the ultrasonic method in Liebermann (1975) up to 0.75 GPa and in Rigden and Jackson (1991) up to 3 GPa, and the average difference of the obtained bulk moduli by these two studies was ~6 GPa.

The derived equation is as follows:

$$K_{T0} = 270.8(300) + 0.343(59)*V_0 + 23.04(269)*EN_{-\text{total}} \quad (3)$$

with K_{T0} in GPa and V_0 in Å^3. The reduced chi-squared value for the regression is 1.6, indicating a good fit, as shown in Fig. 1. When the unit-cell volume of the 4–2 oxide spinels increases, the bulk modulus decreases, which is in general agreement with Anderson and Anderson (1970). As the electronegativity total of the cations increases, the bulk modulus increases, presumably suggesting that the bonds between the cations and oxygens become more covalent.

Fig. 2 shows the differences between the bulk moduli calculated by our model and those determined in the previous section, varying from −10 to 11 GPa and with an average of

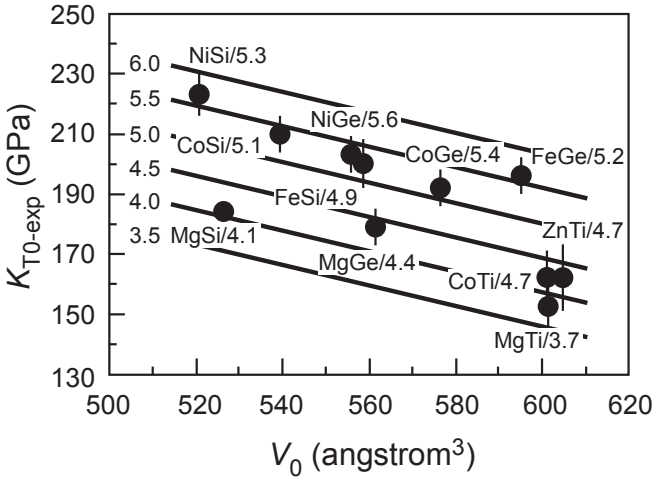

Fig. 1. Calibrating the empirical model (equation (3)). See Table 2 for the plotted data. The model is shown as solid lines numbered with the $EN_{\text{-total}}$ values. The names of the Rw (Mg_2SiO_4 for example) and analogue spinels are abbreviated (MgSi), and followed by their $EN_{\text{-total}}$ values (4.1 for example).

0(7) GPa. Especially, the bulk moduli of the magnesium 4–2 spinels have been perfectly reproduced by our empirical model (difference varying from −2 to 1 GPa only; Table 2), which is in sharp contrast to the poor performance of the theoretical methods (simulated bulk modulus for the Mg_2SiO_4-Rw varying from 173 to 190 GPa; Table 1). On the other hand, the difference for other spinels is relatively larger, presumably reflecting that the cations (Fe, Ni, Co and Zn) in these spinels had multiple charge states, and no all cations were 2+. It follows, anyhow, that our empirical model can well reproduce all experimental data used in its calibration, with an accuracy of about 5% (Table 2).

An independent examination of our model with the data of the Rw solid solutions along the Mg_2SiO_4–Fe_2SiO_4 join has

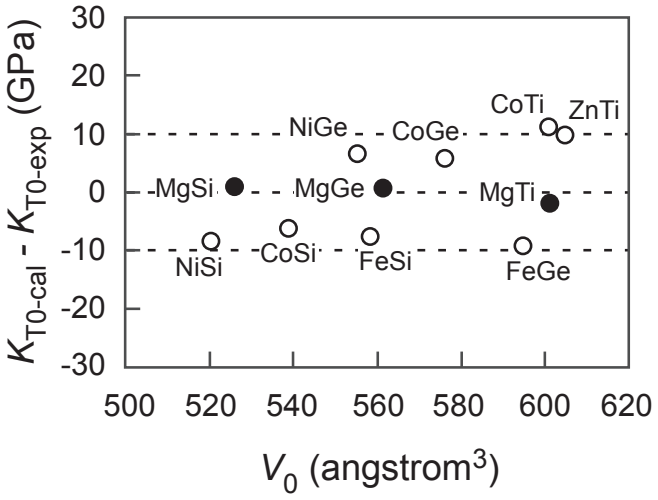

Fig. 2. Difference between the experimentally-estimated isothermal bulk modulus ($K_{T0\text{-exp}}$) and that calculated by our empirical model ($K_{T0\text{-cal}}$; equation (3)). The names of the Rw (Mg_2SiO_4 for example) and analogue spinels are abbreviated (MgSi).

been carried out (Table 2). The result shows that our model can reproduce almost all experimental data well, actually excellent for the $X_{Fe} \leqq 0.5$ samples. Distinctly, the bulk moduli for all iron-rich samples from Hazen (1993) can not be well reproduced, which is probably an issue related to the charge status of the Fe cation, approximately 5% iron occurring as Fe^{3+} in these samples. The effect of Fe^{3+} on the bulk modulus of spinels has not been well constrained though (Yamanaka et al., 2013; Xiong et al., 2015). Since the ringwoodites in the MTZ have X_{Fe} much lower than 0.5, it can be concluded that our empirical model is geologically meaningful.

Our empirical model predicts the bulk modulus of Fe_2TiO_4, Mg_2SnO_4, Co_2SnO_4 and Mn_2SnO_4 as 162, 167, 187 and 166 GPa, respectively. As reviewed in the previous section, the bulk modulus of Fe_2TiO_4 was experimentally determined as 121 GPa by some ultrasonic measurements (Syono et al., 1971; Liebermann et al., 1977) and as 250.8(25) GPa by some high-P X-ray diffraction data (Yamanaka et al., 2009, 2013), both of which were very different to the predicted value. Recently, we remeasured the bulk modulus of Fe_2TiO_4-Sp with a diamond-anvil cell coupled with synchrotron X-ray radiation and obtained 148(4) GPa (K_{T0}' fixed as 4; Xiong et al. (2015)), which closely approached the predicted value of 162 GPa. Considering the iron-rich nature of the Fe_2TiO_4 spinel, this application of our empirical model essentially confirms its earlier application to the ringwoodites along the Mg_2SiO_4–Fe_2SiO_4 join: it has relatively low but still acceptable accuracy at Fe-rich conditions. For the stannates, the experimentally obtained bulk modulus was 125(2), 126(14) and 128(4), respectively (Liebermann et al., 1977), with the ultrasonic measurements conducted up to 0.75 GPa only, which probably resulted in an underestimate of the residual porosity in the samples. In order to resolve the discrepancy, anyhow, more experimental investigations on the stannates are necessary.

5. Solid solution behavior of the ringwoodites in the system Mg_2SiO_4–Fe_2SiO_4 and composition effect on the bulk modulus

At appropriate P-T conditions, a complete series of Rw solid solutions exists in the system Mg_2SiO_4–Fe_2SiO_4. Their volume–composition relationship was demonstrated to obey the Vegard's law (ideal mixing) by some experimental studies (Akimoto and Fujisawa, 1968; Ringwood and Major, 1970; Akimoto, 1972; Suito, 1972; Akaogi et al., 1989). In contrast, the experimental data on the Fe–Mg partitioning between Rw and coexisting phases indicated a non-ideal mixing behavior for the Rw solid solutions (Frost, 2003a, 2003b). As a rule of thumb, a relatively fast crystal structure adjustment and a relatively slow composition modification due to sluggish chemical diffusion should be anticipated to take place during sample-quenching at subsolidus condition, so that a non-ideal solid solution behavior is more likely for the Rw solid solutions.

We have collected 40 unit-cell volume data for the anhydrous ringwoodites (Table 3), and plotted them in Fig. 3(a). In contrast to the observation once made by all early volume-composition studies (Akimoto and Fujisawa, 1968; Ringwood and Major, 1970; Akimoto, 1972; Suito, 1972; Akaogi et al., 1989), a small S-shaped deviation from the Vegard's law is vaguely demonstrated (thin broken curve). Although it is observed in the ringwoodites for the first time, this type of non-ideal volume-mixing behavior, with negative deviation from linearity near the small-volume end-member (Mg_2SiO_4-Rw in our case) and positive deviation near the large-volume end-member (Fe_2SiO_4-Rw in our case), is a general phenomenon rather than an exception for the silicate solid solutions (Newton and Wood, 1980). This implies that the exact mixing behavior in this system still needs to be experimentally characterized in order to accurately thermodynamically describe the Rw. To achieve this goal, several

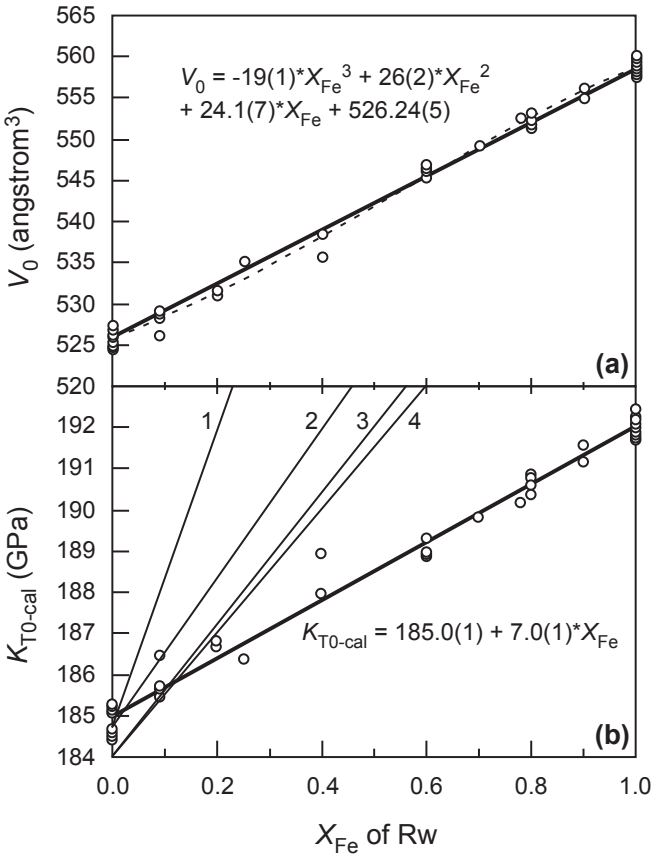

Fig. 3. Correlation between the unit-cell volume (V_0) and composition (X_{Fe}) of the anhydrous ringwoodites (a); Correlation between the calculated isothermal bulk modulus ($K_{T0\text{-}cal}$; equation (3)) and composition (X_{Fe}) of the anhydrous ringwoodites (b). See Table 3 for the sources of the plotted data. The V_0-X_{Fe} relationship can be adequately described with a linear equation (thick solid line; equation (4) in the text). A weighted non-linear equation, displayed as a thin broken curve in (a), results in no significant improvement, and is thus presently rejected. Thin solid lines 1, 2, 3, and 4 in (b) are from Sinogeikin et al. (1998), Liu et al. (2008a), Higo et al. (2006) and Weidner et al. (1984), respectively. The thick solid lines in (a) and (b) represent our final equations (equations (4) and (5)) used in later discussion.

factors such as the water content, the cation order-disorder state and the iron oxidation state have to be simultaneously evaluated along with the X_{Fe} parameter. In addition, in situ measurements should be conducted since the cation order-disorder state may not be fully preserved during sample-quenching (O'Neill et al., 2003). Since the deviation from the Vegard's law is so small and can not be well constrained by the available experimental data, anyhow, we presently choose the following weighted linear equation to describe the volume-composition data in the system Mg_2SiO_4–Fe_2SiO_4:

$$V_0 = 526.26(4) + 31.82(4)*X_{Fe}. \quad (4)$$

Using our empirical model (equation (3)), we next calculate the isothermal bulk moduli of these ringwoodites, and show the result in Fig. 3(b). The resulting equation relating the isothermal bulk modulus and composition of the ringwoodites is:

$$K_{T0-cal} = 185.0(1) + 7.0(1)*X_{Fe}. \quad (5)$$

Compared to the estimates made in Weidner et al. (1984), Sinogeikin et al. (1998), Higo et al. (2006) and Liu et al. (2008a), our result is substantially smaller, by at least 53% (Table 4). Our result thus supports the experimental observation made by Mao et al. (1969) and Nestola et al. (2010), a negligible effect of the Mg/Fe substitution on the bulk modulus of the Rw solid solutions. The much larger composition dependence of the isothermal bulk modulus of the Rw observed in other studies was perhaps caused by some flaws in the employed experimental methods and/or some fluctuations of some microproperties in the investigated samples, as discussed earlier.

6. Sound velocity of the Rw solid solutions in the system Mg_2SiO_4–Fe_2SiO_4

Despite all the potential experimental uncertainties mentioned earlier, it is still highly desirable to directly measure the elastic wave velocities of the Rw solid solutions in the system Mg_2SiO_4–Fe_2SiO_4 by using the ultrasonic method (Li et al., 1996, 1998) or Brillouin scattering technique (Weidner et al., 1984; Sinogeikin et al., 1997, 1998). Such measurements were once made either at high temperature and ambient pressure, or at high pressure and ambient temperature, and inevitably led to some extra uncertainties in the sound velocities at simultaneously high-P and high-T conditions, due to the long distance extrapolation in the P-T space (Li and Liebermann, 2007). Recently, direct sound velocity measurements become possible at P-T conditions generally matching those in the lower part of the MTZ (Higo et al., 2008; Irifune et al., 2008), but the available experimental facilities are still very limited.

Alternatively, the elastic wave velocities (V_s and V_p in km/s) of the Rw at certain P-T condition can be readily calculated by using its corresponding shear modulus (G; GPa), adiabatic bulk modulus (K_S; GPa) and density (ρ; g/cm^3), according to the following equations:

$$V_s = (G/\rho)^{1/2} \quad (6)$$

and

$$V_p = [(K_S + 4/3G)/\rho]^{1/2}. \quad (7)$$

With its G_0, K_{S0} and ρ_0 (G, K_S and ρ at ambient P and T, respectively), $\partial G/\partial T$ and $\partial G/\partial P$, $\partial K_S/\partial T$ and $\partial K_S/\partial P$, and K_{T0}, $\partial K_T/\partial P$ (or K_T') and α well determined, one can probe the influence of P and T on the V_s and V_p. If these parameters are measured for the Rw in a large range of compositions, further, one can simultaneously characterize the effects of P, T and composition, which all are variables in the real Earth.

The effects of the Rw composition on the V_s in the system Mg_2SiO_4–Fe_2SiO_4 at ambient P-T condition, calculated with equation (6), are compared in Fig. 4(a) (Sinogeikin et al., 1998; Higo et al., 2006; Liu et al., 2008a). In general, the result from Liu et al. (2008a) is in good agreement with Higo et al. (2006), which is completely expected from equation (6) and the data listed in Table 4. The absolute (relative)

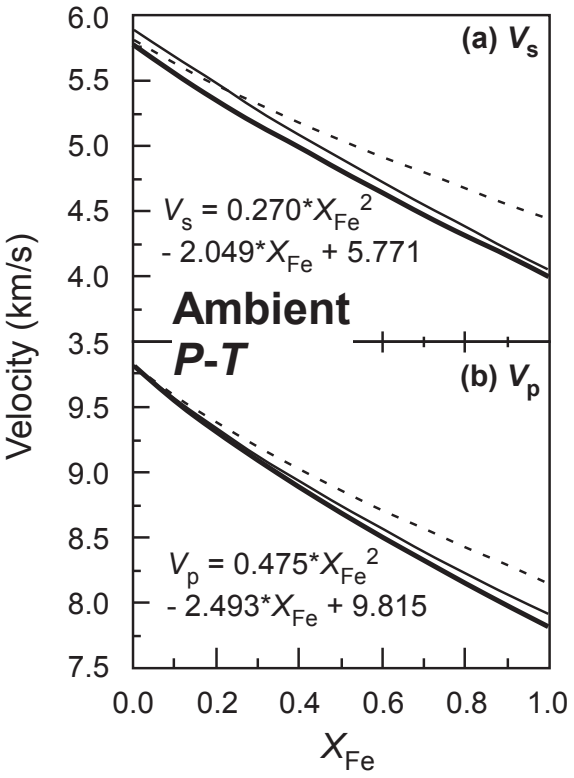

Fig. 4. Effect of Rw composition on the sound velocity at ambient P-T condition: V_s (a) and V_p (b). In the case of the V_s, we calculated the Rw volume with equation (4) and subsequently converted it into density, and calculated the shear modulus with the equation from Sinogeikin et al. (1998) (thin broken curve), Higo et al. (2006) (thin solid curve) or Liu et al. (2008a) (thick solid curve), as listed in Table 4. In the case of the V_p, we calculated the Rw volume with equation (4) and subsequently converted the Rw volume into density, calculated the shear modulus with the equation from Liu et al. (2008a), and calculated the Rw adiabatic/isothermal bulk modulus (ignoring the difference as discussed previously) with the equation from Sinogeikin et al. (1998) (thin broken curve), Higo et al. (2006) (thin solid curve) or this study (equation (5); thick solid curve).

difference in the V_s values between these two studies is very small, from ~0.13 km/s (2%; Mg_2SiO_4-Rw) to 0.04 km/s (1%; Fe_2SiO_4-Rw). The most important point shown in Fig. 4(a) is that the effect of the Rw composition on the V_s is very pronounced, as found in all these studies: when the Rw changes its composition from $X_{Fe} = 0$ to $X_{Fe} = 1$, the overall V_s decrease is ~24% (the thin broken curve), or ~31% (the solid curves). This large composition effect is almost equally contributed by the large variations in the density and shear modulus of the Rw along the join Mg_2SiO_4–Fe_2SiO_4: as the X_{Fe} increases from 0 to 1, the density increases by ~36% whereas the shear modulus decreases by ~21% (Sinogeikin et al., 1998) to 35% (Liu et al., 2008a). Finally, substantial uncertainty still exists in the composition effect on the V_s, due to the difference in the equations describing the Rw composition effect on the shear modulus (Table 4): as the two extreme cases (the thick solid curve versus thin broken curve), the equations from Liu et al. (2008a) and Sinogeikin et al. (1998) result in a relative difference of ~0% in the V_s for the Mg_2SiO_4-Rw, but a relative difference of ~11% for the Fe_2SiO_4-Rw. Considering the similarity of the equations from Weidner et al. (1984), Higo et al. (2006) and Liu et al. (2008a), and the relatively large effect of the Rw composition on the shear modulus (Table 4) which should facilitate an experimental determination with high accuracy, anyhow, we will adopt the latest equation from Liu et al. (2008a) in our later relevant calculations.

The effects of the Rw composition on the V_p in the system Mg_2SiO_4–Fe_2SiO_4 at ambient P-T condition, calculated with equation (7), are shown in Fig. 4(b) (Sinogeikin et al., 1998; Higo et al., 2006; this study). In general, the result from this study is in good agreement with Higo et al. (2006): the absolute (relative) difference in the V_p values between these two studies is very small, from ~0.01 km/s (0%; Mg_2SiO_4-Rw) to 0.11 km/s (1%; Fe_2SiO_4-Rw). Furthermore, the composition effect is very pronounced: when the Rw changes its composition from $X_{Fe} = 0$ to $X_{Fe} = 1$, its V_p decreases by ~17% (the thin broken curve), or by ~21% (the solid curves). This large composition effect is generally prescribed by the variations of the density and shear modulus of the Rw along the join Mg_2SiO_4–Fe_2SiO_4, similar to the V_s case. The increase of the bulk modulus for the entire composition range, varying from ~20% (Sinogeikin et al., 1998), to 10% (Liu et al., 2008a), or to ~4% (this study), also makes its contribution by partially counteracting the effects of the density and shear modulus of the Rw: according to equation (7), a smaller composition effect on the bulk modulus leads to a larger composition effect on the V_p. Consequently, small uncertainty in the composition effect on the V_p still exists due to the difference in the equations describing the correlation between the Rw composition and the bulk modulus from different studies: as the two extreme cases (the thick solid curve versus thin broken curve), the equations from this study and Sinogeikin et al. (1998) result in a difference of ~0% in the V_p for the Mg_2SiO_4-Rw, but a difference of ~5% for the Fe_2SiO_4-Rw. Additionally, the potential influence of those different equations describing the correlation between the Rw composition and shear modulus (Table 4) has been assessed: with the effects of the Rw composition on the bulk modulus and density from this study, we have found that the difference in V_p is ~0% for the Mg_2SiO_4-Rw, but gradually increases to ~4% for the Fe_2SiO_4-Rw.

The effect of the Rw composition on the V_s and V_p in the system Mg_2SiO_4–Fe_2SiO_4 at a typical P-T condition of the lower part of the MTZ (21 GPa and 1800 K) is shown in Fig. 5. The calculation was done with the data listed in Table 5. The composition effect is still very prominent: when the Rw changes its composition from $X_{Fe} = 0$ to $X_{Fe} = 1$, its V_s decreases by ~30% while its V_p decreases by ~19%. If the X_{Fe} of the Rw fluctuates between 0.05 and 0.15, then, the variation of its V_s is ~3% (from 5.55 to 5.36 km/s), and that of its V_p is ~2% (from 10.26 to 10.02 km/s).

7. Compositional variation of the Rw in the MTZ

According to Ringwood (1975), the Earth's upper mantle is peridotitic or pyrolitic, and composed of ~60% olivine (Ol), 30% pyroxenes (orthopyroxene and clinopyroxene) and 10% Al-rich phase (plagioclase, spinel or garnet with increasing depth). In the MTZ (from 410 to 660 km, or from ~14 to 24 GPa), Ol transforms into wadsleyite (Wd) at ~14 GPa and further into Rw at ~17 GPa (*Akaogi* et al., 1989; Katsura and Ito, 1989; Fei et al., 1991), and pyroxenes gradually transform into an Al-deficient garnet (majorite; Mj) and eventually disappear at ~16 GPa (Irifune and Ringwood, 1987), so that

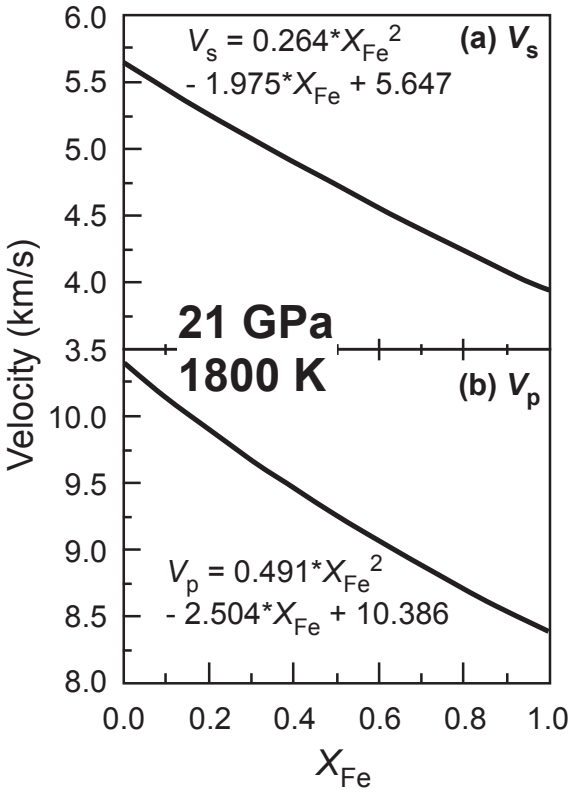

Fig. 5. Effect of Rw composition on the sound velocity at 21 GPa and 1800 K: V_s (a) and V_p (b).

Table 5
Elastic parameters of Rw, used in calculating the sound velocity.

For ambient *P-T* condition							
$G_0 = a + bX_{Fe}$[a]		$K_{T0} = K_{S0} = a + bX_{Fe}$[b]		$V_0 = a + bX_{Fe}$[b]			
a	b	a	b	a	b		
GPa	GPa	GPa	GPa	Å^3	Å^3		
118.7	−41.4	185	7	526.26	31.82		
For high *P*-high *T* condition[c]							
G		K_S		V			
∂G/∂T	∂G/∂P	∂K_S/∂T	∂K_S/∂P	∂K_T/∂T	∂K_T/∂P	$\alpha = a_1 + a_2 (T-T_0)$	
GPa K^{-1}	–	GPa K^{-1}	–	GPa K^{-1}	–	a_1 ($\times 10^{-5}$ K^{-1})	a_2 ($\times 10^{-8}$ K^{-2})
−0.015	1.2	−0.0181	4.33	−0.024	4.34	1.84	1.48

[a] Liu et al. (2008a).
[b] This study.
[c] Higo et al. (2008). Any composition effect on these parameters is secondary and has been ignored in our calculation. Taking the variable ∂K_T/∂T as one example, it was determined as −0.027(5) (Meng et al., 1994), −0.033(4) (Jackson et al., 2000) or −0.029(1) GPa K^{-1} (Katsura et al., 2004) for the Mg_2SiO_4-Rw, as −0.029(3) (Sinogeikin et al., 2003), −0.028(5) (Nishihara et al., 2004), −0.027(1) (Mayama et al., 2005) or −0.024(2) GPa K^{-1} (Higo et al., 2008) for the $(Mg_{0.91}Fe_{0.09})_2SiO_4$-Rw, and as −0.028(1) GPa K^{-1} for the $(Mg_{0.8}Fe_{0.2})_2SiO_4$-Rw (Matsui et al., 2006), indicating its negligible dependence on the Rw composition.

the stable phase assemblage for the pyrolite composition is Wd/Rw (~60%) + Mj (~40%), with slight modification both at low P due to the presence of a small amount of clinopyroxene and at high P due to the presence of a small amount of $CaSiO_3$-rich perovskite (Ca-Pv). Other compositional models such as "piclogite" (a pyroxene- and garnet-rich composition; Anderson and Bass (1986)) were also proposed for the upper mantle, but constantly questioned and less influential in the scientific community (Ita and Stixrude, 1992; Irifune and Isshiki, 1998; Jackson and Rigden, 1998; Li and Liebermann, 2007; Higo et al., 2008; Irifune et al., 2008). The major mineralogical difference between the pyrolite and piclogite composition models is the ratio of the Wd/Rw:Mj: ~6:4 for the former but ~4:6 for the latter (Anderson and Bass, 1986; Duffy and Anderson, 1989).

Although being challenged recently (Cobden et al., 2008), it is commonly accepted that the MTZ of the Earth has rapidly increasing seismic wave velocities with depth according to some seismic reference models such as the PREM (Dziewonski and Anderson, 1981) and AK135 (Kennett et al., 1995). Despite that this feature can put important constraints on the compositional and thermal structure of the MTZ, its origin remains as an unresolved issue: neither pyrolite nor piclogite has been experimentally credited with the potential to explain the steep seismic wave velocity profile in the MTZ (Li and Liebermann, 2007; Irifune et al., 2008). Consequently, some scientists have speculated an origin of potential chemical gradient for the steep seismic wave velocity profile (Duffy and Anderson, 1989; Cammarano and Romanowicz, 2007) whereas others have resorted to a non-adiabatic temperature-depth profile (Cobden et al., 2008).

Rw is the dominant phase in the lower part of the MTZ whether the bulk composition of the upper mantle is of pyrolite or piclogite, and may place important constraints on the steep seismic wave velocity profile in that region. Existing studies demonstrated that compressing Rw along an adiabatic mantle geotherm resulted in much lower sound velocity gradients (Li and Liebermann, 2007; Irifune et al., 2008), compared to those suggested by the seismic reference models like PREM and AK135. Several factors such as the mineral physical data, experimental petrology and solid solution modeling (Helffrich, 2000), however, need to be carefully addressed before solid conclusion can be reached. As illustrated already in this study, the Rw composition effect on the bulk modulus was strongly overestimated (Table 4), which led to a lower V_p gradient according to equation (7). In addition, the excess volume of mixing along the join Mg_2SiO_4–Fe_2SiO_4 was deemed as zero (Akaogi et al., 1989; Ita and Stixrude, 1992; Stixrude and Lithgow-Bertelloni, 2011), but highly possibly not (Fig. 3(a)). The negative excess volume of mixing for the Mg_2SiO_4-rich Rw, especially at $X_{Fe} < 0.2$ which is mostly relevant to the Earth, means that a larger composition effect on the density, and consequently a larger composition effect on the V_s and V_p, should be expected (equations (6) and (7)). Most importantly, the variation pattern of the Rw composition with pressure has never been critically examined for any proposed mantle composition, hampering any further evaluation on the composition effect on the V_s and V_p of the Rw in the lower part of the MTZ.

In total 18 compositional data of Rw have been collected from the high-P experiments with some bulk compositions broadly appropriate for the upper mantle such as the depleted harzburgite with 82 wt% olivine removal (Irifune and Ringwood, 1987), pyrolite (Irifune, 1994), Tinaquillo lherzolite (Wood, 2000), MPY-90 pyrolite (Wood, 2000), K-doped KLB-1 (Wang and Takahashi, 2000), and KLB-1 (Hirose, 2002) at variant P-T conditions, ranging from 19 to 24 GPa and 1573–2373 K (Table 6). The stable phase assemblages observed in these high-P experiments were Rw ± Mj ± Ca-Pv ± Wd ± St (stishovite) ± Mg-Pv ($MgSiO_3$-rich perovskite) ± Mw (magnesiowüstite) ± Ak ($MgSiO_3$-rich akimotoite) ± K phase II ((K,Mg) (Al,Si)O_4 phase) ± Melt. From these high-P experiments, we did not observe any correlation between the X_{Fe} of the Rw and the X_{Fe} of the bulk composition. In order to see the P effect on the composition of the Rw, we removed the data with either too high experimental

Table 6
Compositions of Rw from high-*P* experiments with simulating upper mantle bulk compositions.[a]

Ref.[b]	Bulk composition	Run#	*P*	*T*	Phase assemblage[c]	$X_{Fe\text{-}Rw}$	$X_{Fe\text{-}BC}$
Ref. 1	harzburgite-Ol	MA203	21	1573	Rw + Mj + St	0.090	0.096
Ref. 2	pyrolite	E293	23	1773	Rw + Mj + Ca-Pv	0.090	0.118
		E291	24	1773	Rw + Mj + Ca-Pv + Mg-Pv + Mw	0.099	0.118
Ref. 3	Tinaquillo	55	19	1900	Rw + Mj + Wd	0.112	0.096
	lherzolite	54	22.5	1900	Rw + Mj + Ca-Pv + Mg-Pv + Ox	0.106	0.096
		48	23	1900	Rw + Mj + Ca-Pv + Mg-Pv + Mw	0.100	0.096
	MPY-90 pyrolite	54A	22.5	1900	Rw + Mj + Mg-Pv + Mw	0.100	0.099
Ref. 4	K-doped	3306	20	1673	Rw + Mj + Ca-Pv + K phase II	0.104	0.104
	KLB-1	3312	20	1773	Rw + Mj + Ca-Pv + K phase II	0.119	0.104
		S857	20	1873	Rw + Mj + Melt	0.117	0.104
		S858	20	2373	Rw + Mj + Melt	0.067	0.104
Ref. 5	KLB-1	C132	20.8	2273	Rw + Mj + Ca-Pv + Mw	0.107	0.104
		C188	20.45	2073	Rw + Mj + Ca-Pv	0.101	0.104
		C186	20.9	2073	Rw + Mj + Ca-Pv + Mg-Pv + Mw	0.101	0.104
		C190	20	1873	Rw + Mj + Ca-Pv + Ak + St	0.110	0.104
		C189	20.55	1873	Rw + Mj + Ca-Pv + Mg-Pv	0.112	0.104
		C179	21.45	1873	Rw + Mj + Ca-Pv + Mg-Pv	0.116	0.104
		C187	21.85	1873	Rw + Ca-Pv + Mg-Pv + Mw	0.095	0.104

[a] *P*, pressure in GPa; *T*, temperature in K; $X_{Fe\text{-}Rw}$, atomic ratio Fe/(Fe + Mg) of the Rw; $X_{Fe\text{-}BC}$, atomic ratio Fe/(Fe + Mg) of the bulk composition (BC).
[b] Ref. 1, Irifune and Ringwood (1987); Ref. 2, Irifune (1994); Ref. 3, Wood (2000); Ref. 4, Wang and Takahashi (2000); Ref. 5, Hirose (2002).
[c] Ol, olivine; Rw, ringwoodite; Mj, majorite garnet; St, stishovite; Ca-Pv, $CaSiO_3$-rich perovskite; Mg-Pv, $MgSiO_3$-rich perovskite; Mw, magnesiowustite; Wd, wadslyite; Ox, oxide; K phase II, (K,Mg) (Al,Si)O_4 phase; Ak, akimotoite.

T, or too low experimental *T*, or without Mj phase, and obtained a data set of 6 experiments (Runs E293 and E291 from Irifune (1994), Run 3312 from Wang and Takahashi (2000), and Runs C190, C189 and C179 from Hirose (2002)). A nominally negative correlation between the X_{Fe} of the Rw and the X_{Fe} of the bulk composition emerged, which made no sense and was thus interpreted as an artifice. Since the experimental *T* range was from 1773 to 1873 K only, the real cause to this correlation was pressure, as shown in Fig. 6.

The correlation between the Rw composition and *P* illustrated in Fig. 6 can be described with the following equation:

$$X_{Fe} = 0.222(41) - 0.0053(19)*P \quad (8)$$

where *P* is in GPa (17 < P < 24 GPa). It should be emphasized that this correlation seems neither strongly dependent to the bulk compositions nor severely affected by the temperature in the lower part of the MTZ, which varies by ~50 K only along the normal mantle geotherm from ~17 to 24 GPa (generally ~1773 K at 17 GPa increasing to ~1823 K at 24 GPa; Ito and Katsura, 1989; Jackson, 1998; Jackson and Rigden, 1998). Accordingly, the X_{Fe} of the Rw decreases from ~0.13 to 0.09 as *P* increases from ~17 to 24 GPa. At *P* higher than 24 GPa, Rw breaks down to the phase assemblage Mg-Pv + Mw (Liu, 1976b; Fei et al., 2004).

Several lines of data support the composition variation of the Rw in the lower part of the MTZ, as displayed in Fig. 6. High-*P* experiments in the simple system Mg_2SiO_4–Fe_2SiO_4 demonstrated that the compositions of the Wd-Rw pair moved to the Mg_2SiO_4 end as *P* increased (Ito and Katsura, 1989; Katsura and Ito, 1989; Fei et al., 1991; Frost, 2003b). With the introduction of Mj to the Ol-Wd-Rw system, a negative correlation between the X_{Fe} of the Wd/Mj and *P* was

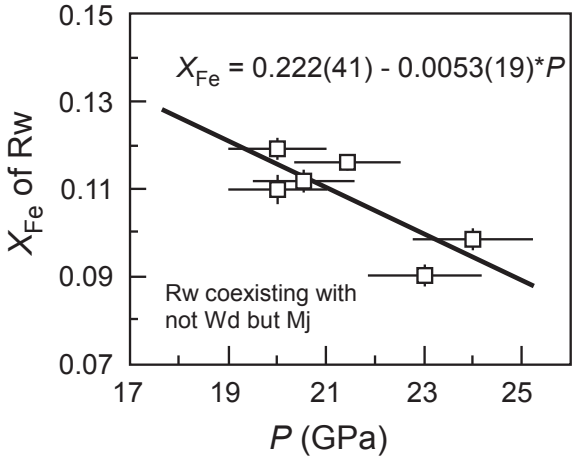

Fig. 6. Correlation of X_{Fe} of Rw and *P* for the pyrolite, KLB-1, and K-doped KLB-1 bulk compositions at 1773 and 1783 K. These temperatures are close to the normal mantle geotherm (Ito and Katsura, 1989; Jackson, 1998; Jackson and Rigden, 1998). Data are from Irifune (1994), Wang and Takahashi (2000), and Hirose (2002). Rw coexists with Mj and $CaSiO_3$-rich perovskite, plus other phases sometimes. Errors in the pressure measurements are assumed as 5%. Errors in the Rw composition (X_{Fe}) reported by Hirose (2002) range from ~0.001 to 0.003, from which an average error, ~0.002, is obtained, and used as an approximate error for the composition data from Irifune (1994) and Wang and Takahashi (2000).

experimentally demonstrated by Irifune and Isshiki (1998); a similar negative correlation between the X_{Fe} of the Rw/Mj and P has not been experimentally demonstrated, but highly possibly remains valid, considering the similar crystal chemical behavior of Rw and Wd in coexistence with Mj (Frost, 2003a, 2003b). Furthermore, Ol inclusions in diamonds from the mantle (Hutchison et al., 2001; Sobolev et al., 2008), with some probably being a retrograde phase of Rw from the lower part of the MTZ (Hutchison et al., 2001), had various X_{Fe} values, from ~0.06 to 0.14, implying a possible correlation between the X_{Fe} and P. To precisely establish such a correlation for the real Earth environment, more quantitative composition and inclusion-formation P data, as documented by Nestola et al. (2011b), should be reported for the natural samples first.

8. Sound velocity features of the Rw in the MTZ

We adopted $X_{Fe} = 0.11$ as the typical composition of the Rw in the MTZ, and calculated with equations (6) and (7) its V_s-P (Fig. 7(a)) and V_p-P (Fig. 7(b)) profiles at 1400, 1600, 1800, 2000 and 2200 K, and along the normal mantle geotherm. The V_s-P profiles at constant T attain the $\partial V_s/\partial P$ values from 0.016 (1400 K) to 0.017 km s^{-1} GPa^{-1} (2200 K) whereas the V_p-P profiles attain the $\partial V_p/\partial P$ values from 0.052 (1400 K) to 0.054 km s^{-1} GPa^{-1} (2200 K). Along the normal mantle geotherm, we find $\partial V_s/\partial P = 0.014$ km s^{-1} GPa^{-1} and $\partial V_p/\partial P = 0.050$ km s^{-1} GPa^{-1}. These values are close to those found at constant T because the T variation along the normal mantle geotherm from 17 to 24 GPa is only ~50 K. The non-shown T effects at constant P are $\partial V_s/\partial T = -0.00029$ (17 GPa) and $\partial V_s/\partial T = -0.00028$ km s^{-1} K^{-1} (23 GPa), and $\partial V_p/\partial T = -0.00037$ km s^{-1} K^{-1} (17 GPa) and $\partial V_p/\partial T = -0.00036$ km s^{-1} K^{-1} (23 GPa). Compared to the V_s-P and V_p-P profiles calculated for the Rw with $X_{Fe} = 0.09$ (Irifune et al., 2008), our profiles have shifted to lower wave velocities mainly due to two factors: one is a larger X_{Fe} value (0.11 versus 0.09), and the other is a smaller G_0 (118.7 GPa from Liu et al. (2008a) vs. 124 GPa from Higo et al. (2006)).

For the pyrolite composition (Ringwood, 1975), the phase assemblage is ~60% Rw + 40% Mj at the lower part of the MTZ. Since both Rw and Mj have $\partial V_s/\partial P$ values from ~0.014 to 0.017 km s^{-1} GPa^{-1} and $\partial V_p/\partial P$ values from ~0.049 to 0.054 km s^{-1} GPa^{-1}, the V_s-P and V_p-P profiles for the pyrolite along the normal mantle geotherm ($\partial V_s/\partial P = 0.014$ and $\partial V_p/\partial P = 0.050$ km s^{-1} GPa^{-1}) are much more gradual than those suggested by the seismic reference models such as the PREM ($\partial V_s/\partial P = 0.054$ and $\partial V_p/\partial P = 0.096$ km s^{-1} GPa^{-1}; Dziewonski and Anderson (1981)) and AK135 ($\partial V_s/\partial P = 0.051$ and $\partial V_p/\partial P = 0.081$ km s^{-1} GPa^{-1}; Kennett et al. (1995)). In order to match these properties, the T dependence of the sound velocities of Rw and Mj would have indicated a low-T anomaly of about 600 K near the 660 km depth if the Rw composition were constant and typically $X_{Fe} = 0.11$ (Fig. 7). It is hard to believe that such a global low-T anomaly exists in the lower part of the normal MTZ. According to Gössler and Kind (1996) and Helffrich (2000), the MTZ beneath continents and oceans are 5 km thicker and 9 km thinner, respectively, suggesting a temperature difference of ~−40 and 70 K only. Only in the regions near subduction zones, low T anomalies generally at the scale of 400−700 K have been predicted to occur in the subducted slabs at the MTZ depths.

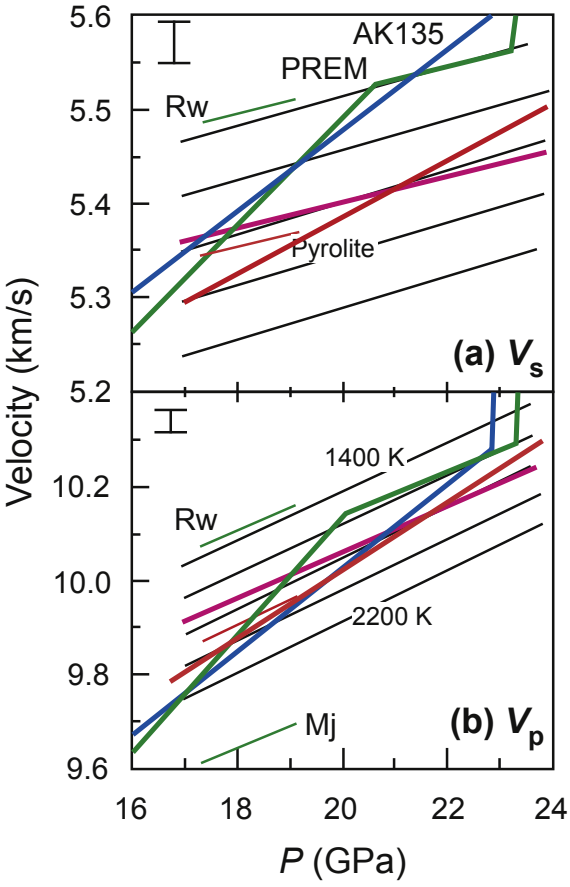

Fig. 7. X_{Fe} effect of the Rw on the V_s-P (a) and V_p-P (b) profiles at the lower part of the MTZ. The thin black lines represent the V_s-P and V_p-P profiles of typical Rw ($X_{Fe} = 0.11$) at constant T (from 1400 to 2200 K) while the thick pink lines stand for the V_s-P and V_p-P profiles along the normal mantle geotherm (~1775−1825 K; Ito and Katsura (1989); Jackson (1998); Jackson and Rigden (1998)). With the X_{Fe} of the Rw decreasing from 0.13 (~17 GPa) to ~0.09 (~24 GPa), the V_s-P and V_p-P profiles become significantly steeper (thick red lines), generally matching within uncertainty the average slops of the seismic velocity profiles suggested by the PREM (thick green curve) and AK135 (thick blue curve) models. Typical errors in this sort of calculation are illustrated both in (a) and (b). For comparison, the V_s-P and V_p-P profiles for Rw with $X_{Fe} = 0.09$ (thin green lines) and pyrolite (~60% Rw with $X_{Fe} = 0.09$ + 40% Mj; thin red lines) at the normal mantle geotherm are also sketched from Irifune et al. (2008). The result for Mj (thin green line) is only shown in (b).

A compositional gradient of the Rw, as shown in Fig. 6, should make a large contribution. Assume the typical composition of the mantle Ol as $X_{Fe} = 0.13$. When the phase transition Wd → Rw completes at ~17 GPa, the Rw attains $X_{Fe} = 0.13$, as required by the mass balance principle. Pressure reduces the X_{Fe} of the Rw to ~0.09 at ~24 GPa (Fig. 6). Taking this compositional variation into account (Fig. 7), the V_s-P and V_p-P profiles of the Rw steepen ($\partial V_s/\partial P = 0.025$ and $\partial V_p/\partial P = 0.064$ km s^{-1} GPa^{-1}), and closely approach the seismic

velocity gradients in the lower part of the MTZ ($\partial V_s/\partial P = 0.054$ and $\partial V_p/\partial P = 0.096$ km s^{-1} GPa^{-1} from the PREM model, and $\partial V_s/\partial P = 0.051$ and $\partial V_p/\partial P = 0.081$ km s^{-1} GPa^{-1} from the AK135 model). A low-T anomaly may still be present at the 660 km depth, but its magnitude required to closely match the gradients of the V_s-P and V_p-P profiles of the Rw with those suggested by the seismic velocity reference models is ~200 K only (Fig. 7), which can be readily explained by the presence of some stagnant slabs along the boundary between the upper mantle and the lower mantle (Fukao et al., 2001).

This raises a series of questions. Is a larger X_{Fe} (0.13) of the Rw at ~17 GPa possible? The only terrestrial occurrence of Rw discovered so far provides a positive answer (its X_{Fe} is ~0.25 with large uncertainty; Pearson et al., 2014). Further, a larger X_{Fe} like ~0.13 for the mantle Ol and its high-P phases should lead to a substantially more complicated picture about the phase transitions in the MTZ. Existing high-P experiment (Ito and Katsura, 1989; Katsura and Ito, 1989; Fei et al., 1991) suggested that the phase transition sequence from low P to high P would be Ol → Ol + Rw → Ol + Wd → Wd → Wd + Rw → Rw. The consequence of these phase transitions on the sound velocity profiles in the upper mantle deserves further exploration, but is out of the scope of this investigation.

Also out of the scope of this investigation is the potential effect of water in the ringwoodites on the V_s-P and V_p-P profiles. Although Rw can host up to ~2.7 wt% water (Kohlstedt et al., 1996; Bolfan-Casanova et al., 2000) and its only terrestrial occurrence contains ~1.4 wt% water (Pearson et al., 2014), some phase equilibrium studies suggested that at the P-T conditions of the MTZ the water solubility of the Rw coexisting with a water-rich melt/fluid phase is mostly limited to ~1 wt% (Ohtani et al., 2000; Litasov and Ohtani, 2003). Consequently, the water content in the Rw in the MTZ with a much lower water fugacity should be much lower. This result is in good agreement with our calculated V_s-P and V_p-P profiles for the anhydrous Rw, which generally match the seismic reference models in magnitudes (Fig. 7). Considering the large reduction effect of water on the sound velocities of Rw (Mao et al., 2012) and the relatively slow sound velocities of Mj (Irifune et al., 2008; as shown in Fig. 7), a large amount of water in the Rw in the normal MTZ, like ~1 wt%, is implausible. As to the water effect on the seismic velocity gradients of V_s-P and V_p-P profiles, the critical point is the variation pattern between the water content in Rw and P, which has not been systematically determined so far. In analogy with the negligible P effect on the water content in Wd at constant T, the water content in Rw presumably would not change significantly with P (Demouchy et al., 2005), leading to a potentially ignorable role of water on the seismic velocity gradients of V_s-P and V_p-P profiles.

9. Conclusion

With complete summarizing and critical analyzing of the relevant experimental data in the literature, we have arrived at the following conclusions:

1. The isothermal bulk modulus of the anhydrous Mg_2SiO_4-Rw, Fe_2SiO_4-Rw and other 4−2 oxide spinels at ambient P-T condition can be approximated by the empirical model $K_{T0} = 270.8(300) + 0.343(59)*V_0 + 23.04(269)*EN_{\text{-total}}$, where K_{T0} is the isothermal bulk modulus in GPa, V_0 the unit-cell volume in Å^3 and $EN_{\text{-total}}$ the total of the electronegativity of all cations in the chemical formula. This model reproduces to an accuracy of ~5% all experimental results used in its construction, and predicts to an accuracy of ~10% the bulk modulus of other 4−2 oxide spinels (Fe_2TiO_4-Sp, for example) not used in the model construction.
2. The available volume-composition data for the Rw solid solutions along the join Mg_2SiO_4–Fe_2SiO_4 vaguely define an extremely small S-shaped curve, with negative deviation from linearity near the Mg_2SiO_4-Rw end and positive deviation near the Fe_2SiO_4-Rw end. They can be well described by the linear equation $V_0 = 526.26(4) + 31.82(4)*X_{Fe}$, anyhow.
3. The composition dependence of the bulk modulus of the Rw solid solutions along the join Mg_2SiO_4–Fe_2SiO_4 can be closely approximated by the equation $K_{T0} = 185.0(1) + 7.0(1)*X_{Fe}$, where X_{Fe} is the atomic ratio Fe/(Fe + Mg) of the Rw. The composition effect on the bulk modulus of the Rw is much smaller than all early determinations.
4. The Rw composition in the lower part of the MTZ of the Earth is not constant, but negatively correlates with P according to the equation $X_{Fe} = 0.2212(41) - 0.0053(19)*P$, where P is pressure in GPa. This correlation is independent to the bulk composition.
5. Taking into account the nearly ideal mixing behavior of the Rw solid solutions, the much smaller composition effect on the Rw bulk modulus, the composition variation of the Rw in the lower part of the MTZ, our calculated V_s-P and V_p-P profiles for Rw show larger gradients, which generally match within uncertainty those constrained by the seismic reference models PREM and AK135. If there is any global low-T anomaly at the depth of 660 km, its required magnitude is not larger than 200 K.

Acknowledgments

We thank Dr Q. Liu for providing some old reference papers and valuable discussions. We thank Dr F. Nestola, Dr M. Walter and an anonymous scientist for commenting on an early version of this manuscript. This investigation was financially supported by the National Natural Science Foundation of China (41273072 and 41090371), the Key Laboratory of Earth's Deep Interior, Chinese Academy of Sciences (DQSB201101), and the State Key Laboratory of Ore Deposit Geochemistry, Institute of Geochemistry, Chinese Academy of Sciences (201114).

References

Akaogi, M., Ito, E., Navrotsky, A., 1989. Olivine-modified spinel-spinel transitions in the system Mg_2SiO_4-Fe_2SiO_4: calorimetric measurements,

thermochemical calculation, and geophysical application. J. Geophys. Res. 94, 15671–15685. http://dx.doi.org/10.1029/JB094iB11p15671.

Akimoto, S., Fujisawa, H., Katsura, T., 1965. The olivine-spinel transition in Fe_2SiO_4 and Ni_2SiO_4. J. Geophys. Res. 70, 1969–1977. http://dx.doi.org/10.1029/JZ070i008p01969.

Akimoto, S., Syono, Y., 1967. High-pressure decomposition for some titanate spinels. J. Chem. Phys. 47, 1813–1817. http://dx.doi.org/10.1063/1.1712170.

Akimoto, S., Fujisawa, H., 1968. Olivine-spinel solid solution equilibria in the system Mg_2SiO_4-Fe_2SiO_4. J. Geophys. Res. 73, 1467–1479. http://dx.doi.org/10.1029/JB073i004p01467.

Akimoto, S., Sato, Y., 1968. High-pressure transformation in Co_2SiO_4 olivine and some geophysical implications. Phys. Earth Planet. Inter. 1, 498–504. http://dx.doi.org/10.1016/0031-9201(68)90018-6.

Akimoto, S., 1972. The system MgO-FeO-SiO_2 at high pressures and temperatures-phase equilibria and elastic properties. Tectonophysics 13, 161–187. http://dx.doi.org/10.1016/0040-1951(72)90019-4.

Anderson, D.L., Anderson, O.L., 1970. The bulk modulus-volume relationship for oxides. J. Geophys. Res. 75, 3494–3500. http://dx.doi.org/10.1029/JZ070i016p03951.

Anderson, D.L., Bass, J.D., 1986. Transition region of the Earth's upper mantle. Nature 320, 321–328. http://dx.doi.org/10.1038/320321a0.

Antao, S.M., Hassan, I., Crichton, W.A., Parise, J.B., 2005. Effects of high pressure and high temperature on cation ordering in magnesioferrite, $MgFe_2O_4$, using in situ synchrotron X-ray powder diffraction up to 1430 K and 6 GPa. Am. Mineral. 90, 1500–1505. http://dx.doi.org/10.2138/am.2005.1797.

Armentrout, M., Kavner, A., 2011. High pressure, high temperature equation of state for Fe_2SiO_4 ringwoodite and implications for the Earth's transition zone. Geophys. Res. Lett. 38, L08309. http://dx.doi.org/10.1029/2011GL046949.

Bartram, S.F., Slepetys, R.A., 1961. Compound formation and crystal structure in the system ZnO-TiO_2. J. Am. Ceram. Soc. 44, 493–499. http://dx.doi.org/10.1111/j.1151-2916.1961.tb13712.x.

Bass, J.D., Weidner, D.J., Hamaya, N., Ozima, M., Akimoto, S., 1984. Elasticity of the olivine and spinel polymorphs of Ni_2SiO_4. Phys. Chem. Mineral. 10, 261–272. http://dx.doi.org/10.1007/BF00311951.

Bolfan-Casanova, N., Keppler, H., Rubie, D.C., 2000. Water partitioning between nominally anhydrous minerals in the MgO-SiO_2-H_2O system up to 24 GPa: implications for the distribution of water in the Earth's mantle. Earth Planet. Sci. Lett. 182, 209–221. http://dx.doi.org/10.1016/S0012-821X(00)00244-2.

Cammarano, F., Romanowicz, B., 2007. Insights into the nature of the transition zone from physically constrained inversion of long-period seismic data. Proc. Natl. Acad. Sci. U. S. A. 104, 9139–9144. http://dx.doi.org/10.1073/pnas.0608075104.

Chang, L., Chen, Z., Liu, X., Wang, H., 2013. Expansivity and compressibility of wadeite-type $K_2Si_4O_9$ determined by in situ high T/P experiments, and their implication. Phys. Chem. Mineral. 40, 29–40. http://dx.doi.org/10.1007/s00269-012-0543-7.

Chopelas, A., Hofmeister, A.M., 1991. Vibrational spectroscopy of aluminate spinels at 1 atm and of $MgAl_2O_4$ to over 200 kbar. Phys. Chem. Mineral. 18, 279–293.

Cobden, L., Goes, S., Cammarano, F., Connolly, J.A.D., 2008. Thermochemical interpretation of one-dimensional seismic reference models for the upper mantle: evidence for bias due to heterogeneity. Geophys. J. Int. 175, 627–648. http://dx.doi.org/10.1111/j.1365-246X.2008.03903.x.

Dachille, F., Roy, R., 1960. High pressure studies of the system Mg_2GeO_4-Mg_2SiO_4 with special reference to the olivine-spinel transition. Am. J. Sci. 258, 225–246.

Datta, R.K., Roy, R., 1967. Equilibrium order-disorder in spinels. J. Am. Ceram. Soc. 50, 578–583. http://dx.doi.org/10.1111/j.1151-2916.1967.tb15002.x.

Demouchy, S., Deloule, E., Frost, D.J., Keppler, H., 2005. Pressure and temperature-dependence of water solubility in Fe-free wadsleyite. Am. Mineral. 90, 1084–1091. http://dx.doi.org/10.2138/am.2005.1751.

Ding, J., Li, D.-Y., Fu, P.-Q., 1990. X-ray powder structural analysis of the spinel polymorph of Fe_2SiO_4. Powder Diffr. 5, 221–222. http://dx.doi.org/10.1017/S0885715600015852.

Dube, G.R., Darshane, V.S., 1991. X-ray, electrical and catalytic studies of the system $CoFe_2O_4$-Co_2TiO_4. Bull. Chem. Soc. Jpn. 64, 2449–2453.

Duffy, T.S., Anderson, D.L., 1989. Seismic velocities in mantle minerals and the mineralogy of the upper mantle. J. Geophys. Res. 94, 1895–1912. http://dx.doi.org/10.1029/JB094iB02p01895.

Dziewonski, A.M., Anderson, D.L., 1981. Preliminary reference Earth model. Phys. Earth Planet. Inter. 25, 297–356. http://dx.doi.org/10.1016/0031-9201(81)90046-7.

Fei, Y., Mao, H.-K., Mysen, B.O., 1991. Experimental determination of element partitioning and calculation of phase relations in the MgO-FeO-SiO_2 system at high pressure and high temperature. J. Geophys. Res. 96, 2157–2169. http://dx.doi.org/10.1029/90JB02164.

Fei, Y., Van Orman, J., Li, J., van Westrenen, W., Sanloup, C., Minarik, W., Hirose, K., Komabayashi, T., Walter, M., Funakoshi, K., 2004. Experimentally determined postspinel transformation boundary in Mg_2SiO_4 using MgO as an internal pressure standard and its geophysical implications. J. Geophys. Res. 109, B02305. http://dx.doi.org/10.1029/2003JB002562.

Finger, L.W., Hazen, R.M., Yagi, T., 1979. Crystal structures and electron densities of nickel and iron silicate spinels at elevated temperature or pressure. Am. Mineral. 64, 1002–1009.

Finger, L.W., Hazen, R.M., Hofmeister, A.M., 1986. High-pressure crystal chemistry of spinel ($MgAl_2O_4$) and magnetite (Fe_3O_4): comparisons with silicate spinels. Phys. Chem. Mineral. 13, 215–220. http://dx.doi.org/10.1007/BF00308271.

Forster, R.H., Hall, E.O., 1965. A neutron and x-ray diffraction study of ulvospinel, Fe_2TiO_4. Acta Crystallogr. 18, 859–862. http://dx.doi.org/10.1107/S0365110X65002104.

Frost, D.J., 2003a. Fe^{2+}-Mg partitioning between garnet, magnesiowüstite, and $(Mg,Fe)_2SiO_4$ phases of the transition zone. Am. Mineral. 88, 387–397.

Frost, D.J., 2003b. The structure and sharpness of $(Mg,Fe)_2SiO_4$ phase transformations in the transition zone. Earth Planet. Sci. Lett. 216, 313–328.

Fukao, Y., Widiyantoro, S., Obayashi, M., 2001. Stagnant slabs in the upper and lower mantle transition region. Rev. Geophys. 39, 291–321. http://dx.doi.org/10.1029/1999RG000068.

Furuhashi, H., Inagaki, M., Naka, S., 1973a. Cation distribution in the solid solutions of the $CoAl_2O_4$-$GeCo_2O_4$ system. J. Inorg. Nucl. Chem. 35, 3707–3711. http://dx.doi.org/10.1016/0022-1902(73)80059-4.

Furuhashi, H., Inagaki, M., Naka, S., 1973b. Determination of cation distribution in spinels by X-ray diffraction method. J. Inorg. Nucl. Chem. 35, 3009–3014. http://dx.doi.org/10.1016/0022-1902(73)80531-7.

Gatta, G.D., Bosi, F., McIntyre, G.J., Hålenius, U., 2014. Static positional disorder in ulvöspinel: a single-crystal neutron diffraction study. Am. Mineral. 99, 255–260. http://dx.doi.org/10.2138/am.2014.4702.

Gössler, J., Kind, R., 1996. Seismic evidence for very deep roots of continents. Earth Planet. Sci. Lett. 138, 1–13. http://dx.doi.org/10.1016/0012-821X(95)00215-X.

Green II, H.W., Chen, W.-P., Brudzinski, M.R., 2010. Seismic evidence of negligible water carried below 410-km depth in subducting lithosphere. Nature 467, 828–831. http://dx.doi.org/10.1038/nature09401.

Hariya, Y., Wai, C.M., 1970. The stability and phase transition of the system Fe_2GeO_4-Fe_2SiO_4. J. Fac. Sci. Hokkaido Univ. 4, 355–363.

Hazen, R.M., 1993. Comparative compressibilities of silicate spinels: anomalous behavior of $(Mg,Fe)_2SiO_4$. Science 259, 206–209. http://dx.doi.org/10.1126/science.259.5092.206.

Hazen, R.M., Downs, R.T., Finger, L.W., Ko, J., 1993. Crystal chemistry of ferromagnesian silicate spinels: evidence for Mg-Si disorder. Am. Mineral. 78, 1320–1323.

Hazen, R.M., Yang, H., 1999. Effects of cation substitution and order-disorder on P-V-T equations of state of cubic spinels. Am. Mineral. 84, 1956–1960.

Helffrich, G., 2000. Topography of the transition zone seismic discontinuities. Rev. Geophys. 38, 141–158. http://dx.doi.org/10.1029/1999RG000060.

He, Q., Liu, X., Hu, X., Deng, L., Chen, Z., Li, B., Fei, Y., 2012. Solid solutions between lead fluorapatite and lead fluorvanadate apatite: compressibility determined by using a diamond-anvil cell coupled with synchrotron X-ray diffraction. Phys. Chem. Mineral. 39, 219–226. http://dx.doi.org/10.1007/s00269-011-0477-5.

He, Q., Liu, X., Li, B., Deng, L., Chen, Z., Liu, X., Wang, H., 2013. Expansivity and compressibility of strontium and barium fluorapatite determined by in situ X-ray diffraction at high-T/P conditions: significance of the M-site cations. Phys. Chem. Mineral. 40, 349–360. http://dx.doi.org/10.1007/s00269-013-0576-6.

Higo, Y., Inoue, T., Li, B., Irifune, T., Liebermann, R.C., 2006. The effect of iron on the elastic properties of ringwoodite at high pressure. Phys. Earth Planet. Inter. 159, 276–285. http://dx.doi.org/10.1016/j.pepi.2006.08.004.

Higo, Y., Inoue, T., Irifune, T., Funakoshi, K., Li, B., 2008. Elastic wave velocities of $(Mg_{0.91}Fe_{0.09})_2SiO_4$ ringwoodite under P-T conditions of the mantle transition region. Phys. Earth Planet. Inter. 166, 167–174. http://dx.doi.org/10.1016/j.pepi.2008.01.003.

Hirose, K., 2002. Phase transitions in pyrolitic mantle around 670-km depth: implications for upwelling of plumes from the lower mantle. J. Geophys. Res. 107, 2078. http://dx.doi.org/10.1029/2001JB000597.

Hofmeister, A.M., Mao, H.K., 2001. Evaluation of shear moduli and other properties of silicates with the spinel structure from IR spectroscopy. Am. Mineral. 86, 622–639.

Holtzclaw Jr., H.F., Robinson, W.R., 1988. General Chemistry. D. C. Heath and Company.

Hutchison, M.T., Hursthouse, M.B., Light, M.E., 2001. Mineral inclusions in diamonds: associations and chemical distinctions around the 670-km discontinuity. Contrib. Mineral. Petrol. 142, 119–126. http://dx.doi.org/10.1007/s004100100279.

Inagaki, M., Ozeki, T., Furuhashi, H., Naka, S., 1977. Solid solubility and cation distribution in the system Co_2GeO_4-Mg_2GeO_4. J. Solid State Chem. 20, 169–172. http://dx.doi.org/10.1016/0022-4596(77)90064-0.

Inoue, T., Weidner, D.J., Northrup, P.A., Parise, J.B., 1998. Elastic properties of hydrous ringwoodite (γ-phase) in Mg_2SiO_4. Earth Planet. Sci. Lett. 160, 107–113. http://dx.doi.org/10.1016/S0012-821X(98)00077-6.

Irifune, T., Ringwood, A.E., 1987. Phase transformation in primitive MORB and pyrolite compositions to 25 GPa and some geophysical implications. In: Manghnani, M., Syono, Y. (Eds.), High-pressure Research in Mineral Physics. Terra/Am. Geophys. Union, Tokyo/Washington, pp. 221–230.

Irifune, T., 1994. Absence of an aluminous phase in the upper part of the Earth's lower mantle. Nature 370, 131–133. http://dx.doi.org/10.1038/370131a0.

Irifune, T., Isshiki, M., 1998. Iron partitioning in a pyrolite mantle and the nature of the 410-km seismic discontinuity. Nature 392, 702–705. http://dx.doi.org/10.1038/33663.

Irifune, T., Higo, Y., Inoue, T., Kono, Y., Ohfuji, H., Funakoshi, K., 2008. Sound velocities of majorite garnet and the composition of the mantle transition region. Nature 451, 814–817. http://dx.doi.org/10.1038/nature06551.

Ita, J., Stixrude, L., 1992. Petrology, elasticity and composition of the mantle transition zone. J. Geophys. Res. 97, 6849–6866. http://dx.doi.org/10.1029/92JB00068.

Ito, E., 1975. High-pressure decompositions in cobalt and nickel silicates. Phys. Earth Planet. Inter. 10, 88–93. http://dx.doi.org/10.1016/0031-9201(75)90022-9.

Ito, E., Matsui, Y., 1979. High-pressure transformations in silicates, germanates, and titanates with ABO_3 stoichiometry. Phys. Chem. Mineral. 4, 265–273. http://dx.doi.org/10.1007/BF00307950.

Ito, E., Katsura, T., 1989. A temperature profile of the mantle transition zone. Geophys. Res. Lett. 16, 425–428. http://dx.doi.org/10.1029/GL016i005p00425.

Jackson, I., 1998. Elasticity, composition and temperature of the Earth's lower mantle: a reappraisal. Geophys. J. Int. 134, 291–311. http://dx.doi.org/10.1046/j.1365-246x.1998.00560.x.

Jackson, I., Rigden, S.M., 1998. Composition and temperature of the Earth's mantle: seismological models interpreted through experimental studies of Earth materials. In: Jackson, I. (Ed.), The Earth's Mantle: Composition, Structure and Evolution. Cambridge Univ. Press, pp. 405–460.

Jackson, J.M., Sinogeikin, S.V., Bass, J.D., 2000. Sound velocities and elastic properties of γ-Mg_2SiO_4 to 873 K by Brillouin spectroscopy. Am. Mineral. 85, 296–303.

Katsura, T., Ito, E., 1989. The system Mg_2SiO_4-Fe_2SiO_4 at high pressures and temperatures: precise determination of stabilities of olivine, modified spinel, and spinel. J. Geophys. Res. 94, 15663–15670. http://dx.doi.org/10.1029/JB094iB11p15663.

Katsura, T., Yokoshi, S., Song, M., Kawabe, K., Tsujimura, T., Kubo, A., Ito, E., Tange, Y., Tomioka, N., Saito, K., Nozawa, A., Funakoshi, K., 2004. Thermal expansion of Mg_2SiO_4 ringwoodite at high pressures. J. Geophys. Res. 109, B12209. http://dx.doi.org/10.1029/2004JB003094.

Kelbert, A., Schultz, A., Egbert, G., 2009. Global electromagnetic induction constraints on transition-zone water content variations. Nature 460, 1003–1007. http://dx.doi.org/10.1038/nature08257.

Kennett, B.L.N., Engdahl, E.R., Buland, R., 1995. Constraints on seismic velocities in the Earth from travel times. Geophys. J. Int. 122, 108–124. http://dx.doi.org/10.1111/j.1365-246x.1995.tb03540.x.

Kiefer, B., Stixrude, L., Wentzcovitch, R.M., 1997. Calculated elastic constants and anisotropy of Mg_2SiO_4 spinel at high pressure. Geophys. Res. Lett. 24, 2841–2844. http://dx.doi.org/10.1029/97GL02975.

Kiefer, B., Stixrude, L., Wentzcovitch, R., 1999. Normal and inverse ringwoodite at high pressures. Am. Mineral. 84, 288–293.

Klotz, S., Chervin, J.-C., Munsch, P., Le Marchand, G., 2009. Hydrostatic limits of 11 pressure transmitting media. J. Phys. D: Appl. Phys. 42, 075413. http://dx.doi.org/10.1088/0022-3727/42/7/075413.

Kohlstedt, D.L., Keppler, H., Rubie, D.C., 1996. Solubility of water in the α, β and γ phases of $(Mg,Fe)_2SiO_4$. Contrib. Mineral. Petrol. 123, 345–357. http://dx.doi.org/10.1007/s004100050161.

Kudoh, Y., Kuribayashi, T., Mizobata, H., Ohtani, E., 2000. Structure and cation disorder of hydrous ringwoodite, γ-$Mg_{1.89}Si_{0.98}H_{0.30}O_4$. Phys. Chem. Mineral. 27, 474–479. http://dx.doi.org/10.1007/s002690000091.

Liebermann, R.C., 1975. Elasticity of olivine (α), beta (β), and spinel (γ) polymorphs of germanates and silicates. Geophys. J. R. Astr. Soc. 42, 899–929.

Liebermann, R.C., Jackson, I., Ringwood, A.E., 1977. Elasticity and phase equilibria of spinel disproportionation reactions. Geophys. J. R. Astr. Soc. 50, 553–586.

Li, B., Gwanmesia, G.D., Liebermann, R.C., 1996. Sound velocity of olivine and beta polymorphs of Mg_2SiO_4 at Earth's transition zone pressures. Geophys. Res. Lett. 23, 2259–2262. http://dx.doi.org/10.1029/96GL02084.

Li, B., Liebermann, R.C., Weidner, D.J., 1998. Elasticity of wadsleyite to 7 GPa and 873 kelvin. Science 281, 675–677. http://dx.doi.org/10.1126/science.281.5377.675.

Li, B., 2003. Compressional and shear wave velocities of ringwoodite γ-Mg_2SiO_4 to 12 GPa. Am. Mineral. 88, 1312–1317.

Li, B., Liebermann, R.C., 2007. Indoor seismology by probing the Earth's interior by using sound velocity measurements at high pressures and temperatures. Proc. Natl. Acad. Sci. U. S. A. 104, 9145–9150. http://dx.doi.org/10.1073/pnas.0608609104.

Li, B., Liebermann, R.C., 2014. Study of the Earth's interior using measurements of sound velocities in minerals by ultrasonic interferometry. Phys. Earth Planet. Inter. 233, 135–153. http://dx.doi.org/10.1016/j.pepi.2014.05.006.

Li, K., Ding, Z., Xue, D., 2011. Electronegativity-related bulk moduli of crystal materials. Phys. Status Solidi B 246, 1227–1236. http://dx.doi.org/10.1002/pssb.201046448.

Li, L., Weidner, D.J., Brodholt, J., Alfe, D., Price, G.D., 2006. Elasticity of Mg_2SiO_4 ringwoodite at mantle conditions. Phys. Earth Planet. Inter. 157, 181–187. http://dx.doi.org/10.1016/j.pepi.2006.04.002.

Litasov, K., Ohtani, E., 2003. Stability of various hydrous phases in CMAS pyrolite-H_2O system up to 25 GPa. Phys. Chem. Mineral. 30, 147–156. http://dx.doi.org/10.1007/s00269-003-0301-y.

Liu, A.Y., Cohen, M.L., 1989. Prediction of new low compressibility solids. Science 245, 841–842. http://dx.doi.org/10.1126/science.245.4920.841.

Liu, L., Bassett, W.A., Takahashi, T., 1974. Isothermal compressions of a spinel phase of Co_2SiO_4 and magnesian ilmenite. J. Geophys. Res. 79, 1171–1174. http://dx.doi.org/10.1029/JB079i008p01171.

Liu, L., 1975a. Disproportionation of Ni_2SiO_4 to stishovite plus bunsenite at high pressures and temperatures. Earth Planet. Sci. Lett. 24, 357–362. http://dx.doi.org/10.1016/0012-821X(75)90141-7.

Liu, L., 1975b. High-pressure disproportionation of Co_2SiO_4 spinel and implications for Mg_2SiO_4 spinel. Phys. Earth Planet. Inter. 25, 286–290. http://dx.doi.org/10.1016/0012-821X(75)90243-5.

Liu, L., 1976a. High-pressure phases of Co_2GeO_4, Ni_2GeO_4, Mn_2GeO_4 and $MnGeO_3$: implications for the germanate-silicate modeling scheme and the Earth's mantle. Earth Planet. Sci. Lett. 31, 393–396. http://dx.doi.org/10.1016/0012-821X(76)90120-5.

Liu, L., 1976b. The post-spinel phases of forsterite. Nature 262, 770–772. http://dx.doi.org/10.1038/262770a0.

Liu, Q., Liu, W., Whitaker, M.L., Wang, L., Li, B., 2008a. Compressional and shear wave velocities of Fe_2SiO_4 spinel at high pressure and high temperature. High Press. Res. 28, 405–413. http://dx.doi.org/10.1080/08957950802296287, 10/2008; 28: 405–413.

Liu, X., Prewitt, C.T., 1990. High-temperature X-ray diffraction study of Co_3O_4: transition from normal to disordered spinel. Phys. Chem. Mineral. 17, 168–172.

Liu, X., O'Neill, C.H.St., Berry, A.J., 2006. Partial melting of spinel lherzolite in the system CaO-MgO-Al_2O_3-SiO_2-H_2O-CO_2-Na_2O at 1.1 GPa. J. Petrol. 47, 409–434. http://dx.doi.org/10.1093/petrology/egi081.

Liu, X., Shieh, S.R., Fleet, M.E., Akhmetov, A., 2008b. High-pressure study on lead fluorapatite. Am. Mineral. 93, 1581–1584. http://dx.doi.org/10.2138/am.2008.2816.

Liu, X., Shieh, S.R., Fleet, M.E., Zhang, L., 2009. Compressibility of a natural kyanite to 17.5 GPa. Prog. Nat. Sci. 19, 1281–1286. http://dx.doi.org/10.1016/j.pnsc.2009.04.001.

Liu, X., Fleet, M.E., Shieh, S.R., He, Q., 2011a. Synthetic lead bromapatite: X-ray structure at ambient pressure and compressibility up to about 20 GPa. Phys. Chem. Mineral. 38, 397–406. http://dx.doi.org/10.1007/s00269-010-0413-0.

Liu, X., Liu, W., He, Q., Deng, L., Wang, H., He, D., Li, B., 2011b. Isotropic thermal expansivity and anisotropic compressibility of ReB_2. Chin. Phys. Lett. 28, 036401. http://dx.doi.org/10.1088/0256-307X/28/3/036401.

Ma, C.B., 1975. Structure refinement of high-pressure Ni_2SiO_4 spinel. Z. Kristallogr. 141, 126–137. http://dx.doi.org/10.1524/zkri.1975.141.1-2.126.

Mao, H.K., Takahashi, T., Bassett, W.A., Weaver, J.S., Akimoto, S., 1969. Effect of pressure and temperature on the molar volumes of wüstite and of three (Fe, $Mg)_2SiO_4$ spinel solid solutions. J. Geophys. Res. 74, 1061–1069. http://dx.doi.org/10.1029/JB074i004p01061.

Mao, H.K., Takahashi, T., Bassett, W.A., 1970. Isothermal compression of the spinel phase of Ni_2SiO_4 up to 300 kilobars at room temperature. Phys. Earth Planet. Inter. 3, 51–53. http://dx.doi.org/10.1016/0031-9201(70)90043-9.

Mao, Z., Lin, J.-F., Jacobsen, S.D., Duffy, T.S., Chang, Y.-Y., Smyth, J.R., Frost, D.J., Hauri, E.H., Prakapenka, V.B., 2012. Sound velocities of hydrous ringwoodite to 16 GPa and 673 K. Earth Planet. Sci. Lett. 331–332, 112–119. http://dx.doi.org/10.1016/j.epsl.2012.03.001.

Matsui, M., 1999. Computer simulation of the Mg_2SiO_4 phases with application to the 410 km seismic discontinuity. Phys. Earth Planet. Inter. 116, 9–18. http://dx.doi.org/10.1016/S0031-9201(99)00119-3.

Matsui, M., Katsura, T., Kuwata, A., Hagiya, K., Tomioka, N., Sugita, M., Yokoshi, S., Nozawa, A., Funakoshi, K., 2006. Equation of state of $(Mg_{0.8},Fe_{0.2})_2SiO_4$ ringwoodite from synchrotron X-ray diffraction up to 20 GPa and 1700 K. Eur. J. Mineral. 18, 523–528. http://dx.doi.org/10.1127/0935-1221/2006/0018-0523.

Mayama, N., Suzuki, I., Saito, T., Ohno, I., Katsura, T., Yoneda, A., 2005. Temperature dependence of the elastic moduli of ringwoodite. Phys. Earth Planet. Inter. 148, 353–359. http://dx.doi.org/10.1016/j.pepi.2004.09.007.

Meng, Y., Fei, Y., Weidner, D.J., Gwanmesia, G.D., Hu, J., 1994. Hydrostatic compression of γ-Mg_2SiO_4 to mantle pressure and 700 K: thermal equation of state and related thermoelastic properties. Phys. Chem. Mineral. 21, 407–412. http://dx.doi.org/10.1007/BF00203299.

Millard, R.L., Peterson, R.C., Hunter, B.K., 1995. Study of the cubic to tetragonal transition in Mg_2TiO_4 and Zn_2TiO_4 spinels by ^{17}O MAS NMR and Rietveld refinement of X-ray diffraction data. Am. Mineral. 80, 885–896.

Miyamoto, Y., Takubo, H., Kume, S., Koizumi, M., 1978. Melting of Mg_2GeO_4 under pressure. Bull. Volcanol. 41–44, 664–669. http://dx.doi.org/10.1007/BF02597392.

Mizukami, S., Ohtani, A., Kawai, N., 1975. High-pressure X-ray diffraction studies on β- and γ-Mg_2SiO_4. Phys. Earth Planet. Inter. 10, 177–182. http://dx.doi.org/10.1016/0031-9201(75)90036-9.

Mizutani, H., Hamano, Y., Ida, Y., Akimoto, S., 1970. Compressional-wave velocities of fayalite, Fe_2SiO_4 spinel, and coesite. J. Geophys. Res. 75, 2741–2747. http://dx.doi.org/10.1029/JB075i014p02741.

Morimoto, N., Tokonami, M., Watanabe, M., Koto, K., 1974. Crystal structures of three polymorphs of Co_2SiO_4. Am. Mineral. 59, 475–485.

Nestola, F., Boffa Ballaran, T., Balic-Zunic, T., Princivalle, F., Secco, L., Dal Negro, A., 2007. Comparative compressibility and structural behavior of spinel $MgAl_2O_4$ at high pressures: the independency on the degree of cation order. Am. Mineral. 92, 1838–1843. http://dx.doi.org/10.2138/am.2007.2573.

Nestola, F., Smyth, J.R., Parisatto, M., Secco, L., Princivalle, F., Bruno, M., Prencipe, M., Dal Negro, A., 2009a. Effects of non-stoichiometry on the spinel structure at high pressure: implications for Earth's mantle mineralogy. Geochimi. Cosmochimi. Acta 73, 489–492. http://dx.doi.org/10.1016/j.gca.2008.11.001.

Nestola, F., Secco, L., Bruno, M., Prencipe, M., Martignago, F., Princivalle, F., Dal Negro, A., 2009b. The effect of non-stoichiometry on the high-temperature behaviour of $MgAl_2O_4$ spinel. Mineral. Mag. 73, 301–306. http://dx.doi.org/10.1180/minmag.2009.073.2.301.

Nestola, F., Boffa Ballaran, T., Koch-Muller, M., Balic-Zunic, T., Taran, M., Olsen, L., Princivalle, F., Secco, L., Lundegaard, L., 2010. New accurate compression data for γ-Fe_2SiO_4. Phys. Earth Planet. Inter. 183, 421–425. http://dx.doi.org/10.1016/j.pepi.2010.09.007.

Nestola, F., Balic-Zunic, T., Koch-Muller, M., Secco, L., Princivalle, F., Parisi, F., Dal Negro, A., 2011a. High-pressure crystal structure investigation of synthetic Fe_2SiO_4 spinel. Mineral. Mag. 75, 2649–2655. http://dx.doi.org/10.1180/minmag.2011.075.5.2649.

Nestola, F., Nimis, P., Ziberna, L., Longo, M., Marzoli, A., Harris, J.W., Manghnani, M.H., Fedortchouk, Y., 2011b. First crystal-structure determination of olivine in diamond: composition and implications for provenance in the Earth's mantle. Earth Planet. Sci. Lett. 305, 249–255. http://dx.doi.org/10.1016/j.epsl.2011.03.007.

Newton, R.C., Wood, B.J., 1980. Volume behavior of silicate solid solutions. Am. Mineral. 65, 733–745.

Nishihara, Y., Takahashi, E., Matsukage, K.N., Iguchi, T., Nakayama, K., Funakoshi, K., 2004. Thermal equation of state of $(Mg_{0.91}Fe_{0.09})_2SiO_4$ ringwoodite. Phys. Earth Planet. Inter. 143–144, 33–46. http://dx.doi.org/10.1016/j.pepi.2003.02.001.

Nunez Valdez, M., Wu, Z., Yu, Y.G., Revenaugh, J., Wentzcovitch, R.M., 2012. Thermoelastic properties of ringwoodite $(Fe_x,Mg_{1-x})_2SiO_4$: its relationship to the 520 km seismic discontinuity. Earth Planet. Sci. Lett. 351–352, 115–122. http://dx.doi.org/10.1016/j.epsl.2012.07.024.

Ohtani, E., 1979. Melting relation of Fe_2SiO_4 up to about 200 kbar. J. Phys. Earth 27, 189–208.

Ohtani, E., Mizobata, H., Yurimoto, H., 2000. Stability of dense hydrous magnesium silicate phases in the systems Mg_2SiO_4-H_2O and $MgSiO_3$-H_2O at pressures up to 27 GPa. Phys. Chem. Mineral. 27, 533–544. http://dx.doi.org/10.1007/s002690000097.

O'Neill, H. St. C., Navrotsky, A., 1983. Simple spinels: crystallographic parameters, cation radii, lattice energies, and cation distribution. Am. Mineral. 68, 181–194.

O'Neill, H. St. C., Redfern, S.A.T., Kesson, S., Short, S., 2003. An in situ neutron diffraction study of cation disordering in synthetic qandilite Mg_2TiO_4 at high temperatures. Am. Mineral. 88, 860–865.

Panero, W.R., 2008. Cation disorder in ringwoodite and its effects on wave speeds in the Earth's transition zone. J. Geophys. Res. 113, B10204. http://dx.doi.org/10.1029/2008JB005676.

Pearson, D.G., Brenker, F.E., Nestola, F., McNeill, J., Nasdala, L., Hutchison, M.T., Matveev, S., Mather, K., Silversmit, G., Schmitz, S., Vekemans, B., Vincze, L., 2014. Hydrous mantle transition zone indicated by ringwoodite included within diamond. Nature 507, 221–224. http://dx.doi.org/10.1038/nature13080.

Piekarz, P., Jochym, P.T., Parlinski, K., Lazewski, J., 2002. High-pressure and thermal properties of γ-Mg_2SiO_4 from first-principles calculations. J. Chem. Phys. 117, 3340–3344. http://dx.doi.org/10.1063/1.1494802.

Rigden, S.M., Jackson, I., Niesler, H., Ringwood, A.E., Liebermann, R.C., 1988. Pressure dependence of the elastic wave velocities from Mg_2GeO_4

spinel to 3 GPa. Geophys. Res. Lett. 15, 605–608. http://dx.doi.org/10.1029/GL015i006p00605.

Rigden, S.M., Jackson, I., 1991. Elasticity of germanate and silicate spinels at high pressure. J. Geophys. Res. 96, 9999–10006. http://dx.doi.org/10.1029/90JB02490.

Ringwood, A.E., 1958. The constitution of the mantle-II. Further data on the olivine-spinel transition. Geochim. Cosmochim. Acta 15, 18–29. http://dx.doi.org/10.1016/0016-7037(58)90005-X.

Ringwood, A.E., 1962. Prediction and confirmation of olivine-spinel transformation in Ni_2SiO_4. Geochim. Cosmochim. Acta 26, 457–469. http://dx.doi.org/10.1016/0016-7037(62)90090-X.

Ringwood, A.E., 1963. Olivine-spinel transformation in cobalt orthosilicate. Nature 198, 79–80. http://dx.doi.org/10.1038/198079a0.

Ringwood, A.E., Major, A., 1970. The system Mg_2SiO_4-Fe_2SiO_4 at high pressures and temperatures. Phys. Earth Planet. Inter. 3, 89–108. http://dx.doi.org/10.1016/0031-9201(70)90046-4.

Ringwood, A.E., 1975. Composition and Petrology of the Earth's Mantle. McGraw-Hill, New York.

Rozenberg, G. Kh., Amiel, Y., Xu, W.M., Pasternak, M.P., Jeanloz, R., Hanfland, M., Taylor, R.D., 2007. Structural characterization of temperature- and pressure-induced inverse↔normal spinel transformation in magnetite. Phys. Rev. B 75, 020102(R).

Sakamoto, N., 1962. Magnetic properties of cobalt titanate. J. Phys. Soc. Jpn. 17, 99–102. http://dx.doi.org/10.1143/JPSJ.17.99.

Sasaki, S., Prewitt, C.T., Sato, Y., Ito, E., 1982. Single-crystal X ray study of γ Mg_2SiO_4. J. Geophys. Res. 87, 7829–7832. http://dx.doi.org/10.1029/JB087iB09p07829.

Sato, Y., 1977. Equation of state of mantle minerals determined through high-pressure X-ray study. In: Manghnani, M.H., Akimoto, S. (Eds.), High Pressure Research: Applications to Geophysics. Academic Press, New York, pp. 307–323.

Sawada, H., 1996. Electron density study of spinels: magnesium titanium oxide (Mg_2TiO_4. Mater. Res. Bull. 31, 355–360. http://dx.doi.org/10.1016/0025-5408(96)00010-4.

Sedler, I.K., Feenstra, A., Peters, T., 1994. An X-ray powder diffraction study of synthetic $(Fe,Mn)_2TiO_4$ spinel. Eur. J. Mineral. 6, 873–885.

Shieh, S.R., Duffy, T.S., Kubo, A., Shen, G., Prakapenka, V.B., Sata, N., Hirose, K., Ohishi, Y., 2006. Equation of state of the postperovskite phase synthesized from a natural $(Mg,Fe)SiO_3$ orthopyroxene. Proc. Natl. Acad. Sci. U. S. A. 103, 3039–3043. http://dx.doi.org/10.1073/pnas.0506811103.

Sinogeikin, S.V., Bass, J.D., Kavner, A., Jeanloz, R., 1997. Elasticity of natural majorite and ringwoodite from the Catherwood meteorite. Geophys. Res. Lett. 24, 3265–3268. http://dx.doi.org/10.1029/97GL03217.

Sinogeikin, S.V., Katsura, T., Bass, J.D., 1998. Sound velocities and elastic properties of Fe-bearing wadsleyite and ringwoodite. J. Geophys. Res. 103, 20819–20825. http://dx.doi.org/10.1029/98JB01819.

Sinogeikin, S.V., Bass, J.D., Katsura, T., 2003. Single-crystal elasticity of ringwoodite to high pressures and high temperatures: implications for the 520 km seismic discontinuity. Phys. Earth Planet. Inter. 136, 41–66. http://dx.doi.org/10.1016/S0031-9201(03)00022-0.

Smyth, J.R., Holl, C.M., Frost, D.J., Jacobsen, S.D., Langenhorst, F., McCammon, C.A., 2003. Structural systematics of hydrous ringwoodite and water in Earth's interior. Am. Mineral. 88, 1402–1407.

Sobolev, N.V., Logvinova, A.M., Zedgenizov, D.A., Pokhilenko, N.P., Kuzmin, D.V., Sobolev, A.V., 2008. Olivine inclusions in Siberian diamonds: high-precision approach to minor elements. Eur. J. Mineral. 20, 305–315. http://dx.doi.org/10.1127/0935-1221/2008/0020-1829.

Stixrude, L., Lithgow-Bertelloni, C., 2011. Thermodynamics of mantle minerals – II. Phase equilibria. Geophys. J. Int. 184, 1180–1213. http://dx.doi.org/10.1111/j.1365-246X.2010.04890.x.

Suito, K., 1972. Phase transitions of pure Mg_2SiO_4 into a spinel structure under high pressures and high temperatures. J. Phys. Earth 20, 225–243.

Syono, Y., Fukai, Y., Ishikawa, Y., 1971. Anomalous elastic properties of Fe_2TiO_4. J. Phys. Soc. Jpn. 31, 471–476. http://dx.doi.org/10.1143/JPSJ.31.471.

Verwey, E.J.W., Heilmann, E.L., 1947. Physical properties and cation arrangement of oxides with spinel structures I. Cation arrangement in spinels. J. Chem. Phys. 15, 174–180. http://dx.doi.org/10.1063/1.1746464.

Von Dreele, R.B., Navrotsky, A., Bowman, A.L., 1977. Refinement of the crystal structure of Mg_2GeO_4 spinel. Acta Crystallogr. B 33, 2287–2288. http://dx.doi.org/10.1107/S056774087700822X.

Wang, J., Sinogeikin, S.V., Inoue, T., Bass, J.D., 2003a. Elastic properties of hydrous ringwoodite. Am. Mineral. 88, 1608–1611.

Wang, S., Liu, X., Fei, Y., He, Q., Wang, H., 2012. In situ high-temperature powder X-ray diffraction study on the spinel solid solutions $(Mg_{1-x}Mn_x)Cr_2O_4$. Phys. Chem. Mineral. 39, 189–198. http://dx.doi.org/10.1007/s00269-011-0474-8.

Wang, W., Takahashi, E., 2000. Subsolidus and melting experiments of K-doped peridotite KLB-1 to 27 GPa: its geophysical and geochemical implications. J. Geophys. Res. 105, 2855–2868. http://dx.doi.org/10.1029/1999JB900366.

Wang, Z., O'Neill, H.S.C., Lazor, P., Saxena, S.K., 2002a. High pressure Raman spectroscopic study of spinel $MgCr_2O_4$. J. Phys. Chem. Solids 63, 2057–2061.

Wang, Z., Saxena, S.K., Zha, C.S., 2002b. In situ x-ray diffraction and Raman spectroscopy of pressure-induced phase transformation in spinel Zn_2TiO_4. Phys. Rev. B 66, 024103. http://dx.doi.org/10.1103/PhysRevB.66.024103.

Wang, Z., Schiferl, D., Zhao, Y., O'Neill, H.St.C., 2003b. High pressure Raman spectroscopy of spinel-type ferrite $ZnFe_2O_4$. J. Phys. Chem. Solids 64, 2517–2523.

Wechsler, B.A., Lindsley, D.H., Prewitt, C.T., 1984. Crystal structure and cation distribution in titanomagnetites $(Fe_{3-x}Ti_xO_4)$. Am. Mineral. 69, 754–770.

Wechsler, B.A., Von Dreele, R.B., 1989. Structure refinements of Mg_2TiO_4, $MgTiO_3$ and $MgTi_2O_5$ by time-of-flight neutron powder diffraction. Acta Crystallogr. B 45, 542–549. http://dx.doi.org/10.1107/S010876818900786X.

Weidner, D.J., Hamaya, N., 1983. Elastic properties of the olivine and spinel polymorphs of Mg_2GeO_4, and evaluation of elastic analogues. Phys. Earth Planet. Inter. 40, 65–70. http://dx.doi.org/10.1016/0031-9201(83)90045-6.

Weidner, D.J., Sawamoto, H., Sasaki, S., Kumazawa, M., 1984. Single-crystal elastic properties of the spinel phase of Mg_2SiO_4. J. Geophys. Res. 89, 7852–7860. http://dx.doi.org/10.1029/JB089iB09p07852.

Weidner, D.J., Ito, E., 1987. Mineral physics constraints on a uniform mantle composition. Geophys. Monogr. 39, 439–446.

Welch, M.D., Cooper, M.A., Hawthorne, F.C., 2001. The crystal structure of brunogeierite, Fe_2GeO_4 spinel. Mineral. Mag. 65, 441–444.

Wilburn, D.R., Bassett, W.A., 1976. Isothermal compression of spinel (Fe_2SiO_4) up to 75 kbar under hydrostatic conditions. High Temp. High Press. 8, 343–348.

Wittlinger, J., Werner, S., Schulz, H., 1998. Pressure-induced order-disorder phase transition of spinel single crystals. Acta Crystallogr. B 54, 714–721. http://dx.doi.org/10.1107/S010876819800161X.

Wood, B.J., 2000. Phase transformations and partitioning relations in peridotite under lower mantle conditions. Earth Planet. Sci. Lett. 174, 341–354. http://dx.doi.org/10.1016/S0012-821X(99)00273-3.

Xiong, Z., Liu, X., Shieh, S.R., Wang, F., Wu, X., Hong, X., Shi, Y., 2015. Equation of state of a synthetic ulvöspinel, $(Fe_{1.94}Ti_{0.03})Ti_{1.00}O_{4.00}$, at ambient temperature. Phys. Chem. Mineral. 42, 171–177. http://dx.doi.org/10.1007/s00269-014-0714-y.

Yagi, T., Marumo, F., Akimoto, S., 1974. Crystal structures of spinel polymorphs of Fe_2SiO_4 and Ni_2SiO_4. Am. Mineral. 59, 486–490.

Yamanaka, T., 1986. Crystal structures of Ni_2SiO_4 and Fe_2SiO_4 as a function of temperature and heating duration. Phys. Chem. Mineral. 13, 227–232. http://dx.doi.org/10.1007/BF00308273.

Yamanaka, T., Mine, T., Asogawa, S., Nakamoto, Y., 2009. Jahn-Teller transition of Fe_2TiO_4 observed by maximum entropy method at high pressure and low temperature. Phys. Rev. B80, 134120. http://dx.doi.org/10.1103/PhysRevB.80.134120.

Yamanaka, T., Kyono, A., Nakamoto, Y., Meng, Y., Kharlamova, S., Struzhkin, V.V., Mao, H.-K., 2013. High-pressure phase transitions of $Fe_{3-x}Ti_xO_4$ solid solution up to 60 GPa correlated with electronic spin transition. Am. Mineral. 98, 736–744. http://dx.doi.org/10.2138/am.2013.4182.

Ye, Y., Brown, D.A., Smyth, J.R., Panero, W.R., Jacobsen, S.D., Chang, Y.-Y., Townsend, J.P., Thomas, S.-M., Hauri, E.H., Dera, P., Frost, D.J., 2012. Compressibility and thermal expansion of hydrous ringwoodite with 2.5(3)

wt% H_2O. Am. Mineral. 97, 573–582. http://dx.doi.org/10.2138/am.2012.4010.

Yong, W., Botis, S., Shieh, S.R., Shi, W., Withers, A.C., 2012. Pressure-induced phase transition study of magnesiochromite ($MgCr_2O_4$) by Raman spectroscopy and X-ray diffraction. Phys. Earth Planet. Inter. 196–197, 75–82.

Yoshino, T., Manthilake, G., Matsuzaki, T., Katsura, T., 2008. Dry mantle transition zone inferred from the conductivity of wadsleyite and ringwoodite. Nature 451, 326–329. http://dx.doi.org/10.1038/nature06427.

Zerr, A., Reichmann, H., Euler, H., Boehler, R., 1993. Hydrostatic compression of γ-($Mg_{0.6}$, $Fe_{0.4}$)$_2SiO_4$ to 50.0 GPa. Phys. Chem. Mineral. 19, 507–509. http://dx.doi.org/10.1007/BF00203192.